EUROPEAN JOURNAL OF PURE AND APPLIED MATHEMATICS
2026, Vol. 19, Issue 1, Article Number 6799
ISSN 1307-5543 – ejpam.com
Published by New York Business Global

Modeling Antibiotic-Resistant Infections at Fractional Order

Anum Zehra[1], Muhammad Farman[2,3,4,*], Aamir Shehzad[2], Aceng Sambas[3,5], Manal Ghannam[6], Mohamed Hafez[7,8]

[1] *Department of Mathematics, Women University Multan, Multan, Pakistan*
[2] *Faculty of Arts and Sciences, Department of Mathematics, Near East University, Northern Cyprus, Turkey*
[3] *Faculty of Informatics and Computing, Universiti Sultan Zainal Abidin, Campus Besut, 22200 Terengganu, Malaysia*
[4] *Research Center of Applied Mathematics, Khazar University, Baku, Azerbaijan*
[5] *Department of Mechanical Engineering, Universitas Muhammadiyah Tasikmalaya, Tamansari Gobras 46196, Indonesia*
[6] *Applied Science Research Center, Applied Science Private University, Amman, Jordan*
[7] *Faculty of Engineering and Quantity Surveying, INTI International University Colleges, Nilai, Malaysia*
[8] *Faculty of Management, Shinawatra University, Pathum Thani, Thailand*

Abstract. Antibiotic resistance is a serious public health problem because it causes increased human morbidity and mortality from resistant diseases. The goal of this study is to better understand the complicated links between antibiotic use and the formation of resistant bacterial strains. A four-state model for community-acquired antibiotic resistance is constructed, which includes both forward and backward mutation processes, as well as an additional compartment for antibiotic supply modified by usage. The model is examined using the context of the hybrid fractional-order derivative. The study analyzes the well-posedness aspects of the hybrid fractional-order model, as well as stability results, with a focus on the use of Volterra-type Lyapunov functions for equilibrium states. The Lipschitz condition guarantees uniqueness, and computational simulations with the Laplace–Adomian decomposition technique investigate the fractional operator's influence. The model's behavior is investigated using sensitivity and chaos analysis of the solution in a bounded domain. Simulation results with a constant proportional Caputo operator demonstrate the impact of different fractional-order values. The study aims to improve understanding of bacterial illnesses by comparing the results with the Caputo fractional operator, supporting observations related to health phenomena. The incorporation of fractional calculus enhances the reliability of the proposed model for improving public health interventions and policies.

2020 Mathematics Subject Classifications: 26A33, 34A08, 92D30
Key Words and Phrases: Antibiotic resistance, infectious diseases, mathematical model, hybrid fractional operator, sensitivity analysis, Laplace–Adomian decomposition method

*Corresponding author.
DOI: https://doi.org/10.29020/nybg.ejpam.v19i1.6799

Email addresses: anum.6484@wum.edu.pk (A. Zehra), farmanlink@gmail.com (M. Farman), aamir.shehzad.1054@gmail.com (A. Shehzad), acenx.bts@gmail.com (A. Sambas), manal.ghannam@neu.edu.tr (M. Ghannam), mohdahmed.hafez@newinti.edu.my (M. Hafez)

1. Introduction

With an immense number of antibiotic resistance genes seen in nature, bacteria have multiple genetics for resistance to antibiotics. Over the past 50 years, as antibacterial medications have been discovered and widely used, the evolution and dissemination of microbes that are resistant to several drugs has accelerated significantly [1]. Long before people started manufacturing antibiotics to prevent disease, bacterial species evolved resistance to them. Because isolated caves and permafrost cores have been shielded from human contamination, they offer perspectives on resistance mechanisms in pre-antibiotic times [2]. One of the major worldwide health concerns that is leading to a great deal of morbidity and mortality is antibiotic resistance. Comprehending its molecular mechanisms can facilitate the development of novel approaches to treating diseases. Antimicrobial must penetrate the bacterial cell envelope in order to reach their target, particularly in double-membraned Gram-negative bacteria. Since many antibiotics are intrinsically resistant to this impermeable cellular membrane, developing new antimicrobial that can pass through the cell envelope is extremely difficult [3]. Antibiotic resistance severely influences diagnostic and the outcome of therapy, leading to failed treatments, expensive alternative medications, increased morbidity and death rates, longer hospital stays, and high healthcare expenses [4]. One urgent requirement in the fight against bacterial infections is the development of novel antibiotics and antimicrobials. With an increase of microorganisms resistant to antibiotics, antibiotic resistance is a global problem. As a result, last-resort antibiotics become less effective and more illnesses develop that don't improve with traditional therapy. The industry's supply of new antibiotics is running low. The importance of battling medication resistance has been highlighted by World Health Day, which has led to further research and strategies to restore treatment choices [5]. Research on animal genetic improvement is essential to lowering antibiotic resistance in microbes. This will assist in finding indicators linked to elevated innate resistance, finding novel antimicrobial drugs, and comprehending how microorganisms contribute to the spread of antibiotic resistance. Current approaches depend on creating next-generation vaccinations and using different bacteriophages or enzymes [6]. For a long time, the real world issues like spread of infectious illnesses has been forecast using mathematical models. Such as the discrete SIS epidemic model [7] and the study of Aamer et al. [8] on the effects of emotional fear, glucose and estrogen excess on cancer and immune system function, mathematical modeling is essential for resolving a variety of life issues. Furthermore, a study by [9] offers a mathematical model for the influence of dust pollution and environmental degradation on the dynamics of plant biomass, indicating that the utilization of plant biomass in greenbelts can successfully lower dust and emissions of greenhouse gases.If the underlying assumptions they make about real-world systems are correct, they can be trusted. Mathematical models can help healthcare providers make better plans and decisions. Epidemiological models aid in sensitive feature management and the prediction of the spread of various bacteria [10–13]. Asymptotic notions are employed in mathematical models to predict the spread of diseases and to impede and ultimately halt the spread of pathogens [14]. Irving, T. J. et al. [15] demonstrated that the combination of seasonal variations in the transmissibility of infection and the transient immunity provided by bacterial carriage might account for the complicated and erratic timing of epidemics. If we are to establish treatment plans for infectious diseases that spread quickly, mathematical modeling will be necessary in the absence of an effective vaccination or

specialist antiviral therapy. When the optimal control plan is implemented as soon as possible, the maximal impact of the disease is dispersed over a longer duration [16].

Because of its memory and genetic characteristics, fractional calculus uses differentiation and integration with fractional order, which makes it more useful than ordinary integer order for modeling phenomena and explaining real-world problems. In many domains, fractional differential equations are essential for depicting real-world situations [17]-[18]. The asymptotic stability of fractional-order differential equations and their general forms for different antibiotics utilized to treat Mycobacterium tuberculosis are examined by Bahatdin Dasbasi [19]. Utilizing the fractal-fractional Mittag-Leffler operator, Farman et al. [20] investigated the qualitative and quantitative aspects of the dynamic behavior of yellow virus in red chilli. To investigate the community dynamics of susceptible, resistant, resilient immunity, and innate cells in an infected person taking several antibiotics and antivirulence medications, a model utilizing fractional-order differential equations is presented in [21]. Using parameter values from the literature, numerical simulations were performed for Pseudomonas aeruginosa and Mycobacterium tuberculosis. Along with antibiotic therapy, the model also examines the impacts of antivirulence medication therapy and how it helps eradicate pathogenic germs. In order to analyze the dynamics of monkeypox viral infection, researchers in [22] created a fractional order model utilizing the Mittag-Leffler kernel. For both endemic and disease-free equilibrium points, they constructed local and global asymptotic stability using a Lyapunov function. Numerical simulations showed that the suggested methods were accurate. According to numerical simulations, the syphilis disease model [23] uses a fractional operator to properly depict complicated interactions that can affect the dynamics of syphilis development and possibly slow its spread in the community. Real data was used to create a fractional-order dynamic model of Methicillin-Resistant Staphylococcus aureus (MRSA) infection in Cyprus [24]. The system was stabilized using Chaos control in accordance with equilibrium points. The model illustrates the stability of treatments and highlights the significance of using antibiotics with awareness in MRSA infections. Using a fractional order model, Ana Koltun et al. [25] examined the interactions among cancer cells, effector immune cells, and the host. They discovered that chemotherapy and other medication treatments have a major effect on the growth of cancer cells. When drug sensitivity and resistance were separated out of the model, it became clear that both variables had a major impact on the rates at which cancer cells proliferate. The study by Alsubaie et al. [26] showed the great benefits of using the Caputo fractional differential operator in an epidemiological model, which led to fewer absolute mean errors and a more accurate depiction of the spread and development of sickness. A thorough understanding of the mechanism of visceral leishmaniasis is provided by the study [27], which uses the fractional Euler method and two fractional-order operators, Caputo-Fabrizio and Atangana-Baleanu, to simulate the disease's dynamics, determine equilibrium points, and identify limited absolute and relative errors. A different study [28] investigates how well the fractional-order SVEIHR influenza model forecasts Saudi Arabia's seasonal influenza outbreaks. It was discovered that whereas immunization increases the rate of virus transmission, vaccination decreases it. A more flexible and generalized operator, the constant-proportional Caputo fractional derivative, was proposed by Baleanu et al. [29]. Additionally, Ali Akgül [30] combined the proportional derivative with two well-known fractional derivatives, producing a number of helpful results based on these definitions as can be

seen in [31–34].

This study provides a fractional order model of antibiotic resistant infections, using newly developed fractional operators to present a new mathematical structure, and examines the results with a focus on treatment default analysis. Our work is novel as it is the first effort to examine such a model using proportional or hybrid fractional derivatives. Because fractional derivatives may reflect long-term dependencies and memory effects, they are useful in models of antibiotic-resistant bacterial diseases. By recognizing the impact of past states on future dynamics, it enables a more accurate depiction of illness development. This advances knowledge of antibiotic resistance, enhances the ability to anticipate treatment outcomes, and facilitates the creation of successful treatment plans. Because it incorporates a variety of memory effects and density-dependent dynamics, the CPC fractional derivative provides more flexibility for models of antibiotic-resistant diseases. This makes it possible to capture intricate behaviors and time-varying dynamics in infectious diseases, such as MRSA or Klebsiella pneumoniae infections, more effectively. It is a potent tool for epidemiological modeling, illness spread prediction, and treatment effectiveness since it expands the capabilities of simpler fractional operators. The structure of the manuscript is as follows: An introduction and a review of the literature are provided in Section 1. In Section 2, we describe the fundamentals of the fractional operator used in the proposed model. In Section 3, we present a fractional order model using hybrid fractional operators for community-based infections that are resistant to antibiotics. Section 4 discusses the sensitivity analysis, the qualitative analysis, and the basic features of the proposed fractional-order model. Section 5 offers more analysis of the suggested operator. In section 6, the model's solution is found using the Laplace-Adomian decomposition method, and several simulations are performed with varying fractional-order values. Sections 7 and 8 discuss the findings and important conclusions of our investigation.

2. Key Concepts

Fractional calculus is crucial for handling mathematical models and understanding the dynamics of complex systems. Its programmable frequency and temporal responses improve performance. The following lists key concepts from fractional calculus that are relevant to our system analysis.

Definition 1. *[29, 35] The Caputo derivative of $\psi(t)$ is defined by*

$$ {}_0^C\mathrm{D}_t^{\varsigma}\psi(t) = \frac{1}{\Gamma(1-\varsigma)}\int_0^t \psi'(\zeta)(t-\zeta)^{-\varsigma}d\zeta. \tag{1}$$

Definition 2. *[29, 35] The Riemann-Liouville (RL) integral is defined by*

$$ {}_0^{RL}\mathrm{I}_t^{\varsigma}\psi(t) = \frac{1}{\Gamma(\varsigma)}\int_0^t (t-\zeta)^{\varsigma-1}\psi(\zeta)d\zeta. \tag{2}$$

Definition 3. *The constant-proportional Caputo (CPC) fractional operator, a hybrid fractional derivative developed by Dumitru Baleanu et al. [29], is given as*

$$ {}_0^{cpc}\mathrm{D}_t^{\varsigma}\psi(t) = \frac{1}{\Gamma(1-\varsigma)}\int_0^t \left[\mathrm{V}_1(\varsigma)\psi(\zeta)+\mathrm{V}_0(\varsigma)\psi'(\zeta)\right](t-\zeta)^{-\varsigma}d\zeta \tag{3}$$

$$= \mathrm{V}_1(\varsigma)\, {}_0^{RL}I_t^{1-\varsigma}\psi(t) + \mathrm{V}_0(\varsigma)\, {}_0^{C}\mathrm{D}_t^{\varsigma}\psi(t). \tag{4}$$

The associated hybrid fractional integral is given by

$${}_0^{cpc}\mathrm{I}_t^{\varsigma}\psi(t) = \frac{1}{\mathrm{V}_0(\varsigma)}\int_0^t \exp\Big\{-\frac{\mathrm{V}_1(\varsigma)}{\mathrm{V}_0(\varsigma)}(t-\zeta)\Big\}{}_0^{RL}\mathrm{D}_{\zeta}^{1-\varsigma}\psi(\zeta)d\zeta \tag{5}$$

Lemma 1. *[29] The CPC derivative's Laplace transform is given as*

$$\mathscr{L}\Big[{}_0^{cpc}\mathrm{D}_t^{\varsigma}\psi(t)\Big] = \Big\{\frac{\mathrm{V}_1(\varsigma)}{s} + \mathrm{V}_0(\varsigma)\Big\}s^{\varsigma}\widehat{\psi}(s) - \mathrm{V}_0 s^{\varsigma-1}\psi(0). \tag{6}$$

3. Model Formulation

Taking into account both forward and backward mutations, Mushanyu [36] developed and examined a four-state community-acquired antibiotic resistance model. Three categories are used to describe the human host population:

- $\mathbf{X}$: Susceptible people;
- $\mathbf{I_s}$: People infected by diseases that are sensitive to antibiotic; and
- $\mathbf{I_r}$: People infected by strains of pathogens that are resistant to antibiotics.

Therefore, the total population of humans is provided by

$$\mathbf{N} = \mathbf{X} + \mathbf{I_s} + \mathbf{I_r}.$$

We further take into account an additional compartment, represented by $\mathbf{A}$, which monitors the antibiotic density over time.

Model's Assumptions:

- In a steady state, the population of susceptible individuals remains constant since the net input of individuals through births or immigration (Λ) is completely balanced by the natural death rate (μ).
- People in class $\mathbf{I_s}$ and class $\mathbf{I_r}$ are thought to be able to only be infected with one strain at a time, assuming that they cannot be superinfected with antibiotic-resistant or sensitive strains, respectively.
- Antibiotics are administered to patients infected with an antibiotic-sensitive strain at a rate of β_a. While a fraction $(1-p)$ of these individuals recover and join class $\mathbf{X}$, a percentage p of them mutate to class $\mathbf{I}_r$.
- Treatment failures in patients infected with antibiotic-sensitive strains or point mutations, which can happen regardless of drug exposure, are examples of a forward mutation process.

- Three outcomes are expected when using antibiotics: either patients with a sensitive strain are cured and go back to class **X**; treatment failure results in antibiotic resistance as patients go from class $\mathbf{I}_s$ to class $\mathbf{I}_r$; or treatment fails without causing resistance, leaving patients with a sensitive strain infection, which is deemed insignificant in this study.

- There is no genetic material transfer through plasmids, the resistance mechanism for infected individuals is based only on mutations, and contact with people infected with a different strain does not change the status of infected individuals.

- With deaths excluded, the net migration rate of people from class $\mathbf{I}_r$ is represented by the parameter σ. Some of these people, q, go via backward mutation to rejoin class $\mathbf{I}_s$, while the others, $(1-q)$, move to class **X** as they naturally eliminate resistant bacteria through their immune response.

- Primary antibiotic-resistant (ABR) instances are modeled by assuming that, once acquired resistance manifests, individuals with resistant strains can pass these on to susceptible individuals. β and $(1-c)\beta$, respectively, reflect the effective contact rates for spreading antibiotic-sensitive and antibiotic-resistant strains. The parameter c, $0 < c < 1$, denotes the fitness cost incurred by bacterial strains as a result of their reduced ability to reproduce or compete.

- The number of infected people at any given time t is correlated with the increase in antibiotic density in supply chains, assuming a direct proportionality. While antibiotic consumption happens at a constant per capita rate μ_a, the contact rates for sensitive and resistant infected people are represented by α_s and α_r, respectively.

A fractional model for bacterial disease incorporates memory effects and non-Markovian dynamics, which are factors that are not taken into account by conventional integer-order models. This allows fractional-order differential equations to more correctly replicate the progression of the disease. Because it is nonlocal, fractional calculus is being used more and more in science, engineering, and mathematics. It is an essential tool in many domains because it enables the realistic simulation of genuine occurrences that depend on both the past and present time history. The nonlinear fractional differential equations given below are used to build the new fractional-order bacterial illness model under the constant-proportional Caputo (CPC) type fractional derivative with $0 < \alpha \leq 1$.

$$\begin{cases} {}^{cpc}{}_0D_t^{\varsigma}\mathbf{X}(t) &= \Lambda + (1-\rho)\beta_a\mathbf{A}\mathbf{I}_s + (1-q)\sigma\mathbf{I}_r - \beta\mathbf{X}\mathbf{I}_s - (1-c)\beta\mathbf{X}\mathbf{I}_r - \mu\mathbf{X}, \\ {}^{cpc}{}_0D_t^{\varsigma}\mathbf{I}_s(t) &= \beta\mathbf{X}\mathbf{I}_s + q\sigma\mathbf{I}_r - \beta_a\mathbf{A}\mathbf{I}_s - (\delta_s+\mu)\mathbf{I}_s, \\ {}^{cpc}{}_0D_t^{\varsigma}\mathbf{I}_r(t) &= (1-c)\beta\mathbf{X}\mathbf{I}_r + \rho\beta_a\mathbf{A}\mathbf{I}_s - (\delta_r+\sigma+\mu)\mathbf{I}_r, \\ {}^{cpc}{}_0D_t^{\varsigma}\mathbf{A}(t) &= \alpha_s\mathbf{I}_s + \alpha_r\mathbf{I}_r - \mu_a\mathbf{A}. \end{cases} \tag{7}$$

where the initial conditions are

$$\mathbf{X}(0) = \mathbf{X}_0 \geq 0, \quad \mathbf{I_s}(0) = \mathbf{I_{s_0}} \geq 0, \quad \mathbf{I_r}(0) = \mathbf{I}_{r_0} \geq 0, \quad \mathbf{A}(0) = \mathbf{A}_0 \geq 0. \tag{8}$$

Fractional derivatives improve the model of community-associated bacterial illnesses by incorporating memory effects and impacting present and future states. This enables a more detailed representation of complicated multi-scale dynamics, a more realistic depiction of disease transmission, and seamless transitions between different modelling scenarios, resulting in more effective public health interventions. The dynamical system is depicted in Figure (1).

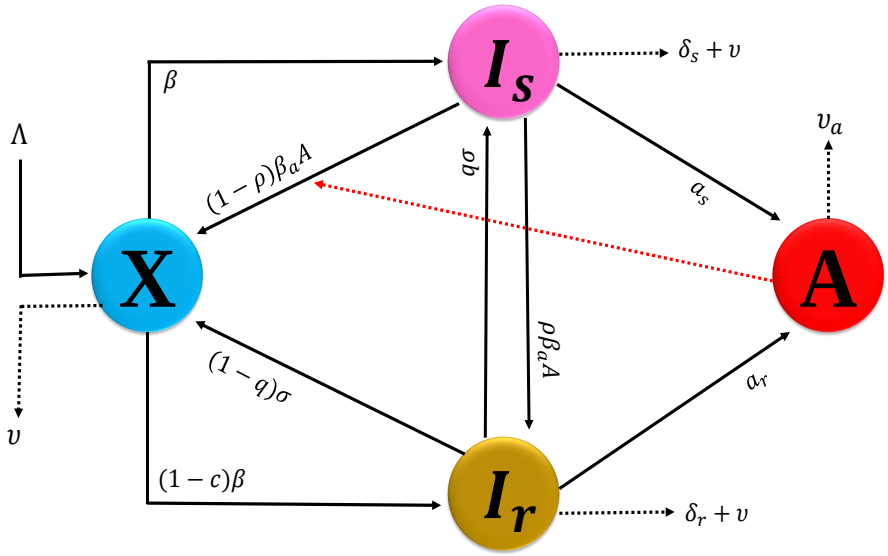

Figure 1: The flow chart illustrates for model formulation.

All the parameters taken into consideration for the model under investigation are compiled in Table 1.

Table 1: Description of model parameters

Parameter	Description
Λ	Net inflow of people due to immigration or births
β	Contact rate between $\mathbf{X}$ and infectious people that increase the antibiotic-sensitive strain
c	The intrinsic fitness cost of bacterial strains
β_a	Rate of antibiotic therapy among patients with an antibiotic-sensitive strain
ρ	A percentage of people go through a forward mutation process to join the class $\mathbf{I}_r$.
q	A percentage of people who go through a backward mutation process to join the class $\mathbf{X}$.
μ	Natural death rate
σ	Net rate of people leaving the class $\mathbf{I}_r$ that disregards factors relating to death.
α_s	The person-antibiotic-supply contact rates for the class $\mathbf{I}_s$
α_r	The person-antibiotic-supply contact rates for the class $\mathbf{I}_r$
μ_a	Per capita antibiotics consumption rate
δ_s	Death rate of antibiotic-sensitive strain
δ_r	Death rate of antibiotic-resistant strain

4. Basic Analysis

This section investigates the constraints that ensure the proposed model's solutions are positive, limited, and well-posed, while assuming relevant real-world conditions. For this purpose, we first define a norm as

$$\|\mathsf{Q}\|_\infty = \sup_{t\in D_{\mathsf{Q}}}|\mathsf{Q}(t)|, \tag{9}$$

where $\mathsf{Q} = \{\mathbf{X}, \mathbf{I_s}, \mathbf{I_r}, \mathbf{A}\}$. We have

$$\begin{aligned}
{}^{cpc}{}_0D_t^{\varsigma}\mathbf{X}(t) &= \Lambda + (1-\rho)\beta_a\mathbf{A}\mathbf{I}_s + (1-q)\sigma\mathbf{I}_r - \beta\mathbf{X}\mathbf{I}_s - (1-c)\beta\mathbf{X}\mathbf{I}_r - \mu\mathbf{X},\\
&\geq -\big(\beta\mathbf{I}_s + (1-c)\beta\mathbf{I}_r + \mu\big)\mathbf{X},\\
&\geq -\big(\beta\sup_{t\in D_{\mathbf{I_s}}}|\mathbf{I}_s| + (1-c)\beta\sup_{t\in D_{\mathbf{I_r}}}|\mathbf{I}_r| + \mu\big)\mathbf{X},\\
&= -\big(\beta||\mathbf{I}_s||_\infty + (1-c)\beta||\mathbf{I}_r||_\infty + \mu\big)\mathbf{X}.
\end{aligned} \tag{10}$$

The above inequality must be resolved in order to derive a lower bound for $\mathbf{X}(t)$. Such inequalities are difficult to solve since the CPC derivative is a hybrid operator. An exponential function is not directly inverted by this. However, it is known that exponentials may be used in solutions for the proportional case, which is a component of CPC. The exponential kernel of the CPC integral (5) really suggests that solutions may have exponential components. Similarly, the exponential-type bound can be obtained by using the hybrid definition to translate to the corresponding first-order ODE. Equation below is therefore probably a bound or an approximation rather than an exact one.

$$\mathbf{X}(t) \geq \mathbf{X}_0\ \exp\Big[-\frac{\mathrm{V}_1(\varsigma)}{\mathrm{V}_0(\varsigma)}(\beta||\mathbf{I}_s||_\infty + (1-c)\beta||\mathbf{I}_r||_\infty + \mu)t\Big] \quad , \quad \forall t \geq 0. \tag{11}$$

$${}^{cpc}{}_0D_t^{\varsigma}\mathbf{I}_s(t) = \beta\mathbf{X}\mathbf{I}_s + q\sigma\mathbf{I}_r - \beta_a\mathbf{A}\mathbf{I}_s - (\delta_s+\mu)\mathbf{I}_s,$$

$$\begin{aligned} &\geq -\big(\beta_a\mathbf{A}-\beta\mathbf{X}+\delta_s+\mu\big)\mathbf{I}_s,\\ &\geq -\big(\beta_a\sup_{t\in D_\mathbf{A}}|\mathbf{A}|-\beta\sup_{t\in D_\mathbf{X}}|\mathbf{X}|+\delta_s+\mu\big)\mathbf{I}_s,\\ &= -\big(\beta_a||\mathbf{A}||_\infty-\beta||\mathbf{X}||_\infty+\delta_s+\mu\big)\mathbf{I}_s. \end{aligned} \tag{12}$$

This implies that

$$\mathbf{I}_s(t)\geq \mathbf{I}_{s_0}\ \exp\Big[-\frac{\mathrm{V}_1(\varsigma)}{\mathrm{V}_0(\varsigma)}(\beta_a||\mathbf{A}||_\infty-\beta||\mathbf{X}||_\infty+\delta_s+\mu)t\Big]\quad,\quad \forall t\geq 0. \tag{13}$$

$$\begin{aligned} {}^{cpc}{}_0D_t^\varsigma\mathbf{I}_r(t) &= (1-c)\beta\mathbf{X}\mathbf{I}_r+\rho\beta_a\mathbf{A}\mathbf{I}_s-(\delta_r+\sigma+\mu)\mathbf{I}_r,\\ &\geq -\big(\delta_r+\sigma+\mu-(1-c)\beta\mathbf{X}\big)\mathbf{I}_r,\\ &\geq -\big(\delta_r+\sigma+\mu-(1-c)\beta\sup_{t\in D_\mathbf{X}}|\mathbf{X}|\big)\mathbf{I}_r,\\ &= -\big(\delta_r+\sigma+\mu-(1-c)\beta||\mathbf{X}||_\infty\big)\mathbf{I}_r. \end{aligned} \tag{14}$$

Therefore,

$$\mathbf{I}_r(t)\geq \mathbf{I}_{r_0}\ \exp\Big[-\frac{\mathrm{V}_1(\varsigma)}{\mathrm{V}_0(\varsigma)}(\delta_r+\sigma+\mu-(1-c)\beta||\mathbf{X}||_\infty)t\Big]\quad,\quad \forall t\geq 0. \tag{15}$$

Likewise, we get

$$\mathbf{A}(t)\geq \mathbf{A}_0\ \exp\Big[-\frac{\mathrm{V}_1(\varsigma)}{\mathrm{V}_0(\varsigma)}(\mu_a)t\Big]\quad,\quad \forall t\geq 0. \tag{16}$$

Lemma 2. *The hybrid fractional order model, (7), is distinct and constrained in addition to the initial conditions.*

Proof.
We get

$$\begin{aligned} {}^{cpc}{}_0D_t^\varsigma\mathbf{X}(t)\Big|_{\mathbf{X}=0} &= \{\Lambda+(1-\rho)\beta_a\mathbf{A}\mathbf{I}_s+(1-q)\sigma\mathbf{I}_r\}\ \geq\ 0,\\ {}^{cpc}{}_0D_t^\varsigma\mathbf{I}_s(t)\Big|_{\mathbf{I_s}=0} &= \{q\sigma\mathbf{I}_r\}\ \geq\ 0,\\ {}^{cpc}{}_0D_t^\varsigma\mathbf{I}_r(t)\Big|_{\mathbf{I_r}=0} &= \{\rho\beta_a\mathbf{A}\mathbf{I}_s\}\ \geq\ 0,\\ {}^{cpc}{}_0D_t^\varsigma\mathbf{A}(t)\Big|_{\mathbf{A}=0} &= \{\alpha_s\mathbf{I}_s+\alpha_r\mathbf{I}_r\}\ \geq\ 0. \end{aligned} \tag{17}$$

Developing a new model for antibiotic-resistant infection requires that the domain be positive invariant and have unique solutions for every compartment, which is demonstrated by the solution's inability (17) to escape from the hyperplane.
Now let

$$Z(t)=\{\mathbf{X}(t)+\mathbf{I}_s(t)+\mathbf{I}_r(t),\ \mathbf{A}(t)\},$$

and

$${}^{cpc}{}_0D_t^\varsigma Z(t)={}^{cpc}{}_0D_t^\varsigma\{\mathbf{X}(t)+\mathbf{I}_s(t)+\mathbf{I}_r(t),\ \mathbf{A}(t)\},$$

Let $\mathbf{X}(t)+\mathbf{I}_s(t)+\mathbf{I}_r(t)=N(t)$ then we have

$$\begin{aligned} {}^{cpc}{}_0D_t^{\varsigma}N(t) &= {}^{cpc}{}_0D_t^{\varsigma}\Big\{\mathbf{X}(t)+\mathbf{I}_s(t)+\mathbf{I}_r(t)\Big\} \\ &\leq \Lambda-\mu N(t) \qquad for\ N\leq\frac{\Lambda}{\mu}, \end{aligned} \tag{18}$$

$$\begin{aligned} {}^{cpc}{}_0D_t^{\varsigma}\mathbf{A}(t) &= \alpha_s\mathbf{I}_s+\alpha_r\mathbf{I}_r-\mu_a\mathbf{A} \\ &\leq (\alpha_s+\alpha_r)\Lambda-\mu_a\mathbf{A}, \qquad for\ \mathbf{A}\leq\frac{(\alpha_s+\alpha_r)\Lambda}{\mu\mu_a} \quad with \quad \Lambda=\mathbf{I}_s+\mathbf{I}_r. \end{aligned} \tag{19}$$

This suggests that ${}^{cpc}{}_0D_t^{\varsigma}Z(t)\leq 0$ and one can find that as $t\to\infty$

$$0 \leq \{\mathbf{X}(t)+\mathbf{I}_s(t)+\mathbf{I}_r(t),\ \mathbf{A}(t)\} \leq \left\{\frac{\Lambda}{\mu},\ \frac{(\alpha_s+\alpha_r)\Lambda}{\mu\mu_a}\right\} \tag{20}$$

Hence, we can investigate our suggested system in the following domain (Υ) that is biologically feasible.

$$\Upsilon=\left\{(\mathbf{X},\ \mathbf{I}_s,\ \mathbf{I}_r,\ \mathbf{A})\in\mathbb{R}_+^4\ :\ N(t)\leq\frac{\Lambda}{\mu},\ \mathbf{A}\leq\frac{(\alpha_s+\alpha_r)\Lambda}{\mu\mu_a}\right\}. \tag{21}$$

5. Qualitative Analysis

5.1. Existence and Uniqueness Analysis

In this section, we will use the fixed point theory. The system (7) can be written as follows:

$$\begin{cases} {}^{cpc}{}_0\mathrm{D}_t^{\varsigma}\psi(t) = \lambda\big(t,\psi(t)\big), \\ \psi(0) = \psi_0\geq 0. \end{cases} \tag{22}$$

where λ is a continuous function vector provided that:

$$\begin{pmatrix}\lambda_1\\ \lambda_2\\ \lambda_3\\ \lambda_4\end{pmatrix}=\begin{pmatrix}\Lambda+(1-\rho)\beta_a\mathbf{A}\mathbf{I}_s+(1-q)\sigma\mathbf{I}_r-\beta\mathbf{X}\mathbf{I}_s-(1-c)\beta\mathbf{X}\mathbf{I}_r-\mu\mathbf{X},\\ \beta\mathbf{X}\mathbf{I}_s+q\sigma\mathbf{I}_r-\beta_a\mathbf{A}\mathbf{I}_s-(\delta_s+\mu)\mathbf{I}_s,\\ (1-c)\beta\mathbf{X}\mathbf{I}_r+\rho\beta_a\mathbf{A}\mathbf{I}_s-(\delta_r+\sigma+\mu)\mathbf{I}_r,\\ \alpha_s\mathbf{I}_s+\alpha_r\mathbf{I}_r-\mu_a\mathbf{A}.\end{pmatrix}, \tag{23}$$

and $\psi(t)=(\mathbf{X},\ \mathbf{I}_s,\ \mathbf{I}_r,\ \mathbf{A})^{\mathrm{T}}$ denotes the system variables with initial conditions $\psi_0=(\mathbf{X}_0,\ \mathbf{I}_{s_0},\ \mathbf{I}_{r_0},\ \mathbf{A}_0)^{\mathrm{T}}$. Also, λ is locally Lipschitz on Υ (21), i.e., there exists $\mathbb{E}\in\mathbb{R}$, such that

$$\Big\|\lambda\big(t,\psi_1(t)\big)-\lambda\big(t,\psi_2(t)\big)\Big\|\leq\mathbb{E}\big\|\psi_1(t)-\psi_2(t)\big\|. \tag{24}$$

Theorem 1. *If*

$$\frac{\mathbb{E}\chi_{\max}^{\varsigma}\tau_{\max}^{\varsigma}}{\mathrm{V}_0(\varsigma)\Gamma(1-\varsigma)}<1\ , \quad t\in[0,\infty), \tag{25}$$

then the hybrid fractional-order system (7) has a unique solution.

Proof. From (5), we can find

$$\psi(t) = \psi(t_0) + \frac{1}{V_0(\varsigma)} \int_0^t \exp\big(-\frac{V_1(\varsigma)}{V_0(\varsigma)}(t-\zeta)\big) {}_0^{RL}D_\zeta^{1-\varsigma} \lambda(\zeta, \psi(\zeta)) d\zeta. \tag{26}$$

Now, let $\varpi = (0, \mathbb{T})$ and $\mathsf{H} : Z(\varpi, \mathbb{R}_+^4) \to Z(\varpi, \mathbb{R}_+^4)$. Then

$$\mathsf{H}\psi(t) = \psi(t_0) + \frac{1}{V_0(\varsigma)} \int_0^t \exp\big(-\frac{V_1(\varsigma)}{V_0(\varsigma)}(t-\zeta)\big) {}_0^{RL}D_\zeta^{1-\varsigma} \lambda(\zeta, \psi(\zeta)) d\zeta. \tag{27}$$

$$\Rightarrow \psi(t) = \mathsf{H}\psi(t). \tag{28}$$

Now, assume that $\|*\|_\varpi$ is the supremum norm on K. Then

$$\|\psi(t)\|_\varpi = \sup_{t\in\varpi} \|\psi(t)\|, \qquad \psi(t) \in Z(\varpi, \mathbb{R}_+^4). \tag{29}$$

Therefore, $Z(\varpi, \mathbb{R}_+^4)$ is a Banach space with $\|*\|_\varpi$. This suggests that

$$\|\int_0^t \upsilon(t,\zeta) d\zeta\| \ \leq \ \|\upsilon(t,\zeta)\|_\varpi \, \|\psi(s)\|_\varpi. \tag{30}$$

where $\psi(t) \in Z(\varpi, \mathbb{R}_+^4)$, and $\upsilon(t,\zeta) \in Z(\varpi^2, \mathbb{R}_+^4)$ which produces

$$\|\upsilon(t,\zeta)\|_\varpi = \sup_{t,\zeta\in\varpi} |\upsilon(t,\zeta)\|. \tag{31}$$

This implies that

$$\begin{aligned}
&\|\mathsf{H}\psi_1(t) - \mathsf{H}\psi_2(t)\|_\varpi \\
&\quad \leq \Big\| \frac{1}{V_0(\varsigma)} \int_0^t \exp\big(\frac{-V_1(\varsigma)}{V_0(\varsigma)}(t-\zeta)\big) \big[{}_0^{RL}D_\zeta^{1-\varsigma}\ \lambda(\zeta, \psi_1(\zeta)) - {}_0^{RL}D_\zeta^{1-\varsigma}\ \lambda(\zeta, \psi_2(\zeta))\big] d\zeta \Big\|_\varpi \\
&\quad \leq \frac{\chi_{\max}^\varsigma}{V_0(\varsigma)\Gamma(1-\varsigma)} \Big\| \int_0^t (t-\zeta)^{\varsigma-2} \big[\lambda(\zeta, \psi_1(\zeta)) - \lambda(\zeta, \psi_2(\zeta))\big] d\zeta \Big\|_\varpi \\
&\quad \leq \frac{\chi_{\max}^\varsigma \tau_{\max}^\varsigma}{V_0(\varsigma)\Gamma(1-\varsigma)} \Big\| \lambda(\zeta, \psi_1(\zeta)) - \lambda(\zeta, \psi_2(\zeta)) \Big\|_\varpi \\
&\quad \leq \frac{\mathbb{E}\chi_{\max}^\varsigma \tau_{\max}^\varsigma}{V_0(\varsigma)\Gamma(1-\varsigma)} \|\psi_1(t) - \psi_2(t)\|_\varpi.
\end{aligned} \tag{32}$$

Hence,

$$\|\mathsf{H}\psi_1(t) - \mathsf{H}\psi_2(t)\|_\varpi \ \leq \ \mathscr{D} \|\psi_1(t) - \psi_2(t)\|_\varpi, \tag{33}$$

where $\mathscr{D} = \frac{\mathbb{E}\chi_{\max}^\varsigma \tau_{\max}^\varsigma}{V_0(\varsigma)\Gamma(1-\varsigma)}$. For $\mathscr{D} < 1$, H is a contraction.

5.2. Equilibrium points and Reproductive Number

By solving the following problem, the equilibrium points of the proposed system (7) can be determined.

$$\begin{aligned} 0 &= \Lambda+(1-\rho)\beta_a\mathbf{A}\mathbf{I}_s+(1-q)\sigma\mathbf{I}_r-\beta\mathbf{X}\mathbf{I}_s-(1-c)\beta\mathbf{X}\mathbf{I}_r-\mu\mathbf{X},\\ 0 &= \beta\mathbf{X}\mathbf{I}_s+q\sigma\mathbf{I}_r-\beta_a\mathbf{A}\mathbf{I}_s-(\delta_s+\mu)\mathbf{I}_s,\\ 0 &= (1-c)\beta\mathbf{X}\mathbf{I}_r+\rho\beta_a\mathbf{A}\mathbf{I}_s-(\delta_r+\sigma+\mu)\mathbf{I}_r,\\ 0 &= \alpha_s\mathbf{I}_s+\alpha_r\mathbf{I}_r-\mu_a\mathbf{A}. \end{aligned} \tag{34}$$

5.2.1. Bacteria-free equilibrium

We have the Bacteria-free equilibrium as follows:

$$P_1 = \left\{\mathbf{X}^0,\, \mathbf{I}_s^0,\, \mathbf{I}_r^0,\, \mathbf{A}^0\right\} = \left\{\frac{\Lambda}{\mu},\, 0,\, 0,\, 0\right\}, \tag{35}$$

5.2.2. Reproductive Number

Following up on our earlier investigation, we will now determine the reproductive number. In the subject of epidemiological modeling, reproduction number is crucial since it aids in understanding the stability requirements. Consider the system

$$\begin{aligned} {}^{cpc}{}_0D_t^{\varsigma}\mathbf{I}_s(t) &= \beta\mathbf{X}\mathbf{I}_s+q\sigma\mathbf{I}_r-\beta_a\mathbf{A}\mathbf{I}_s-(\delta_s+\mu)\mathbf{I}_s,\\ {}^{cpc}{}_0D_t^{\varsigma}\mathbf{I}_r(t) &= (1-c)\beta\mathbf{X}\mathbf{I}_r+\rho\beta_a\mathbf{A}\mathbf{I}_s-(\delta_r+\sigma+\mu)\mathbf{I}_r,\\ {}^{cpc}{}_0D_t^{\varsigma}\mathbf{A}(t) &= \alpha_s\mathbf{I}_s+\alpha_r\mathbf{I}_r-\mu_a\mathbf{A}. \end{aligned} \tag{36}$$

Using the next generation matrix method, we get the basic reproductive number (R_0) as

$$F=\begin{pmatrix} \frac{\beta\Lambda}{\mu} & 0 & 0\\ 0 & \frac{(1-c)\beta\Lambda}{\mu} & 0\\ 0 & 0 & 0 \end{pmatrix}, \quad V=\begin{pmatrix} \delta_s+\mu & -q\sigma & 0\\ 0 & \delta_r+\sigma+\mu & 0\\ -\alpha_s & -\alpha_r & \mu_a 0 \end{pmatrix}, \tag{37}$$

$$V^{-1}=\begin{pmatrix} \frac{1}{\delta_s+\mu} & \frac{q\sigma}{(\delta_s+\mu)(\delta_r+\sigma+\mu)} & 0\\ 0 & \frac{1}{\delta_r+\sigma+\mu} & 0\\ \frac{\alpha_s}{\mu_a(\delta_s+\mu)} & \frac{\alpha_r}{\mu_a(\delta_s+\mu)(\delta_r+\sigma+\mu)} & \frac{1}{\mu_a} \end{pmatrix}. \tag{38}$$

According to the next generation matrix approach, the dominating eigenvalue is the long-term growth factor of an epidemic since it shows how quickly the next generation of infected people will spread. Then, from

$$|FV^{-1}-\Lambda I|=0, \tag{39}$$

we get the dominant eigenvalue known as reproductive number (R_0) by

$$\mathrm{R}_0 = \mathrm{R}_{\mathrm{I}_s}+\mathrm{R}_{\mathrm{I}_r}, \tag{40}$$

where

$$\mathrm{R}_{\mathrm{I}_s} = \frac{\beta\Lambda}{\mu(\delta_s+\mu)} \tag{41}$$

$$\mathrm{R}_{\mathrm{I}_r} = \frac{(1-c)\beta\Lambda}{\mu(\delta_r+\sigma+\mu)}. \tag{42}$$

To improve estimates and take into consideration different disease dynamics, the reproductive number (R_0) computations are made simpler. To concentrate on the effects of interventions, time-dependent characteristics such as transmission rates are separated. In order to keep model complexity and uncertainty from overpowering transmission indications, parameters that are challenging to measure-particularly in the early phases of an outbreak-are removed.

5.2.3. Bacteria-persistent equilibrium

Following three potential endemic equilibria are identified by calculating bacteria-persistent equilibrium points for system (7):

- Bacteria-sensitive only equilibrium:

$$P_2 = \left\{\mathbf{X}^{\odot}, \mathbf{I}_s^{\odot}, \mathbf{I}_r^{\odot}, \mathbf{A}^{\odot}\right\}, \tag{43}$$

where

$$\mathbf{X}^{\odot} = \frac{\mu_a\delta_s^2+\Lambda\beta_a\alpha_s}{\beta\mu_a\delta_s+\mu\beta_a\alpha_s}, \qquad \mathbf{I}_s^{\odot} = \frac{\mu\mu_a\delta_s}{\beta\mu_a\delta_s+\mu\beta_a\alpha_s}\left(\frac{\beta\Lambda-\mu(\delta_s+\mu)}{\mu(\delta_s+\mu)}\right),$$
$$\mathbf{I}_r^{\odot} = 0, \qquad \mathbf{A}^{\odot} = \frac{\mu\alpha_s\delta_s}{\beta\mu_a\delta_s+\mu\beta_a\alpha_s}\left(\frac{\beta\Lambda-\mu(\delta_s+\mu)}{\mu(\delta_s+\mu)}\right). \tag{44}$$

- Bacteria-resistant only equilibrium:

$$P_3 = \left\{\mathbf{X}^{\otimes}, \mathbf{I}_s^{\otimes}, \mathbf{I}_r^{\otimes}, \mathbf{A}^{\otimes}\right\}, \tag{45}$$

where

$$\mathbf{X}^{\otimes} = \frac{\delta_r}{(1-c)\beta}, \qquad \mathbf{I}_r^{\otimes} = \frac{\mu\delta_r}{(1-c)\beta(\mu+\delta_r)}\left(\frac{(1-c)\beta\Lambda-\mu(\delta_r+\sigma+\mu)}{\mu(\delta_r+\sigma+\mu)}\right),$$
$$\mathbf{I}_s^{\otimes} = 0, \qquad \mathbf{A}^{\otimes} = \frac{\mu\alpha_r\delta_r}{\mu_a(1-c)\beta(\mu+\delta_r)}\left(\frac{(1-c)\beta\Lambda-\mu(\delta_r+\sigma+\mu)}{\mu(\delta_r+\sigma+\mu)}\right). \tag{46}$$

- Internal endemic equilibrium is

$$P_4 = \left\{\mathbf{X}^*, \mathbf{I}_s^*, \mathbf{I}_r^*, \mathbf{A}^*\right\}, \tag{47}$$

where

$$\mathbf{X}^* = \frac{\Lambda+(1-\rho)\beta_a\mathbf{A}^*\mathbf{I}_s^*+(1-q)\sigma\mathbf{I}_r^*}{\beta\mathbf{I}_s^*+(1-c)\beta\mathbf{I}_r^*+\mu}, \qquad \mathbf{I}_s^* = \frac{q\sigma\mathbf{I}_r^*}{\beta_a\mathbf{A}^*+\delta_s+\mu-\beta\mathbf{X}^*},$$
$$\mathbf{I}_r^* = \frac{\rho\beta_a\mathbf{A}^*\mathbf{I}_s^*}{(\delta_r+\sigma+\mu)-(1-c)\beta\mathbf{X}^*}, \qquad \mathbf{A}^* = \frac{\alpha_s\mathbf{I}_s^*+\alpha_r\mathbf{I}_r^*}{\mu_a}. \tag{48}$$

5.3. Sensitivity analysis of R_0

In epidemiological modeling, sensitivity analysis evaluates how certain parameters affect R_0. By methodically altering the model's parameters sensitivity analysis of a reproductive number identifies which have the most effects on the R_0's value and, consequently, the spread of disease. To determine the most important components, this analysis is carried out by varying the input parameter values within their likely ranges and paying attention to the changes in the R_0 output that result. In order to lower R_0 and control the disease, parameters with high negative sensitivity indices-such as treatment/recovery rates-are essential. By analyzing how parameters affect important variables, sensitivity testing evaluates the stability of the model. The R_0 sensitivity can be examined by examining the partial derivative of thresholds.

- For R_{I_s}, we have

$$\begin{aligned} \frac{\partial R_{I_s}}{\partial \beta} &= \frac{\Lambda}{\mu(\delta_s+\mu)} > 0, & \frac{\partial R_{I_s}}{\partial \Lambda} &= \frac{\beta}{\mu(\delta_s+\mu)} > 0, \\ \frac{\partial R_{I_s}}{\partial \mu} &= -\frac{\beta\Lambda(2\mu+\delta_s)}{\mu^2(\delta_s+\mu)^2} < 0, & \frac{\partial R_{I_s}}{\partial \delta_s} &= -\frac{\beta\Lambda}{\mu(\delta_s+\mu)^2} < 0. \end{aligned} \tag{49}$$

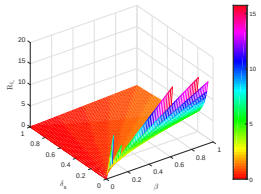

(a) R_{I_s}'s variations with δ_s and β

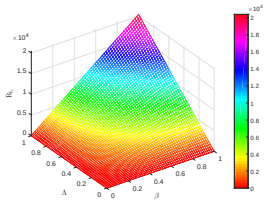

(b) R_{I_s}'s variations with Λ and β

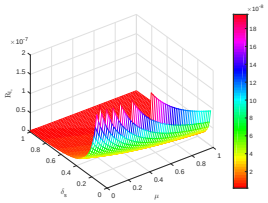

(c) R_{I_s}'s variations with δ_s and μ

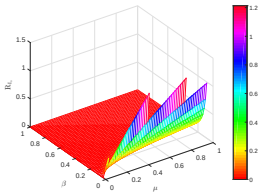

(d) R_{I_s}'s variations with μ and β

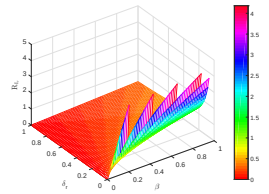

(e) R_{I_r}'s variations with δ_r and β

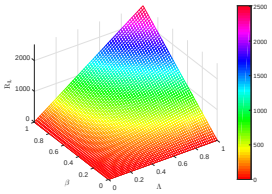

(f) R_{I_r}'s variations with β and Λ

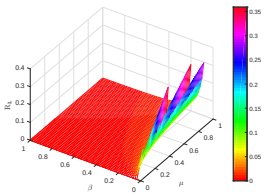

(g) R_{I_r}'s variations with μ and β

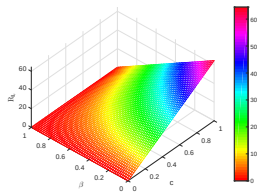

(h) R_{I_r}'s variations with β and c

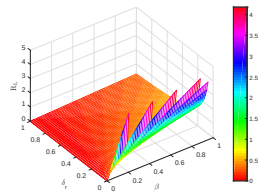

(i) R_{I_r}'s variations with c and δ_r

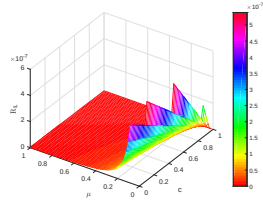

(j) R_{I_r}'s variations with c and μ

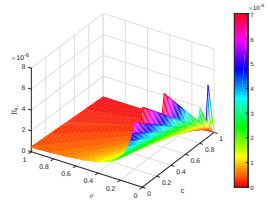

(k) R_{I_r}'s variations with σ and c

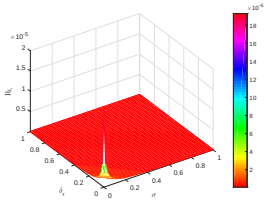

(l) R_{I_r}'s variations with σ and δ_r

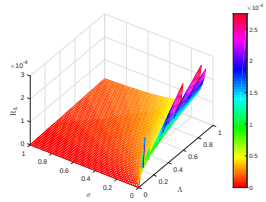

(m) R_{I_r}'s variations with σ and Λ

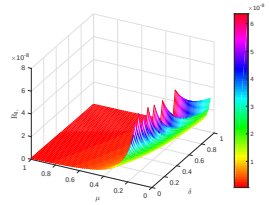

(n) R_{I_r}'s variations with σ and δ_r

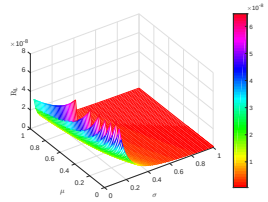

(o) R_{I_r}'s variations with σ and μ

Figure 2: The sensitivity analysis of R_{I_s} and R_{I_r} to the parameters

- For $\mathrm{R}_{\mathrm{I}_r}$, we obtain

$$\begin{aligned}
\frac{\partial \mathrm{R}_{\mathrm{I}_r}}{\partial c} &= -\frac{\beta\Lambda}{\mu(\delta_r+\sigma+\mu)} < 0, & \frac{\partial \mathrm{R}_{\mathrm{I}_r}}{\partial \beta} &= \frac{(1-c)\Lambda}{\mu(\delta_r+\sigma+\mu)} > 0,\\
\frac{\partial \mathrm{R}_{\mathrm{I}_r}}{\partial \Lambda} &= \frac{(1-c)\beta}{\mu(\delta_r+\sigma+\mu)} > 0, & \frac{\partial \mathrm{R}_{\mathrm{I}_r}}{\partial \sigma} &= -\frac{(1-c)\beta\Lambda}{\mu(\delta_r+\sigma+\mu)^2} < 0,\\
\frac{\partial \mathrm{R}_{\mathrm{I}_r}}{\partial \mu} &= -\frac{(1-c)\beta\Lambda(\delta_r+\sigma+2\mu)}{\mu^2(\delta_r+\sigma+\mu)^2} < 0, & \frac{\partial \mathrm{R}_{\mathrm{I}_r}}{\partial \delta_r} &= -\frac{(1-c)\beta\Lambda}{\mu(\delta_r+\sigma+\mu)^2} < 0.
\end{aligned} \tag{50}$$

Increasing a parameter value results in an increase in R_0, according to a positive sensitivity index, whilst decreasing R_0 is indicated by a negative sensitivity index. Through simulations, as shown in Figure (2), these techniques assist in identifying important factors affecting the risk of illness spreading and associated effects. R_0 rises, for instance, when the contact rate β rises. Disease transmission is more likely at higher contact rates. Additionally, R_0 drops as bacterial species' intrinsic fitness costs rise. The stability of a resistant strain is significantly influenced by the size of the fitness cost. There is selective pressure against the resistant strain when antibiotic use is decreased because the fitness cost becomes more noticeable. Public health experts can prioritize efforts by determining which criteria have the greatest impact on R_0. For example, reducing transmission becomes a key concern if the transmission rate has a high positive sensitivity.

5.4. Local Stability

Theorem 2. *Bacteria-free equilibrium* (P_1) *is locally stable if* $\mathrm{R}_{\mathrm{I}_s} < 1$ *and* $\mathrm{R}_{\mathrm{I}_r} < 1$.

Proof. We calculate the Jacobian matrix of the system (7) at the equilibrium point (P_1) as

$$J(P_1) = \begin{bmatrix} -\mu & -\frac{\beta\Lambda}{\mu} & -q\sigma - c\frac{\beta\Lambda}{\mu} & 0\\ 0 & \frac{\beta\Lambda}{\mu} - (\delta_s+\mu) & 0 & 0\\ 0 & 0 & -c\frac{\beta\Lambda}{\mu} - (\delta_r+\sigma+\mu) & 0\\ 0 & \alpha_s & \alpha_r & -\mu_a \end{bmatrix}. \tag{51}$$

The characteristic equation is calculated as

$$C(\xi) = \begin{vmatrix} \xi+\mu & \frac{\beta\Lambda}{\mu} & q\sigma + c\frac{\beta\Lambda}{\mu} & 0\\ 0 & \xi + (\delta_s+\mu) - \frac{\beta\Lambda}{\mu} & 0 & 0\\ 0 & 0 & \xi + (\delta_r+\sigma+\mu) + c\frac{\beta\Lambda}{\mu} & 0\\ 0 & -\alpha_s & -\alpha_r & \xi+\mu_a \end{vmatrix}, \tag{52}$$

where

$$\begin{aligned}
\xi_1 &= -\mu, & \xi_2 &= -(\delta_s+\mu) + \frac{\beta\Lambda}{\mu},\\
\xi_3 &= -(\delta_r+\sigma+\mu) - c\frac{\beta\Lambda}{\mu}, & \xi_4 &= -\mu_a.
\end{aligned} \tag{53}$$

All the eigenvalues are negative or < 0, hence the equilibrium point (P_1) is stable.

5.5. Global Stability

For the analysis of global stability of our bacterial-resistant infection model (7), we explore the following results.

Lemma 3. *For all $t \geq t_0$, a continuous function $\mathrm{M} \in \mathbb{R}^4_+$ satisfies:*

$$ {}^{cpc}_{0}\mathrm{D}^{\varsigma}_{t}\left(\mathrm{M}-\mathrm{M}^{*}-\mathrm{M}^{*}\ln\frac{\mathrm{M}}{\mathrm{M}^{*}}\right) \leq \left(1-\frac{\mathrm{M}^{*}}{\mathrm{M}}\right){}^{cpc}_{0}\mathrm{D}^{\varsigma}_{t}\mathrm{M}(t), \quad \mathrm{M}^{\bullet} \in \mathbb{R}^{+}, \forall \varsigma \in (0,1). \tag{54}$$

Theorem 3. *If $\mathrm{R}_{\mathrm{I}_s} < 1$ and $\mathrm{R}_{\mathrm{I}_r} < 1$, the bacteria-free equilibrium point, denoted by P_1, of the fractional-order system (7) is globally asymptotically stable.*

Proof. We define the Lyapunov function as

$$\mathrm{H}(t) \;=\; (\mathbf{X}-\mathbf{X}^{0}-\mathbf{X}^{0}\ln\frac{\mathbf{X}}{\mathbf{X}^{0}})+\mathbf{I}_s+\mathbf{I}_r+\mathbf{A}. \tag{55}$$

From (7), we get

$${}^{cpc}\mathrm{D}^{\varsigma}_{t}\mathrm{M}(t) \;\leq\; (\frac{\mathbf{X}-\mathbf{X}^{0}}{\mathbf{X}}){}^{cpc}_{0}\mathrm{D}^{\varsigma}_{t}\mathbf{X} \;+\; {}^{cpc}_{0}\mathrm{D}^{\varsigma}_{t}\mathbf{I}_s \;+\; {}^{cpc}_{0}\mathrm{D}^{\varsigma}_{t}\mathbf{I}_r \;+\; {}^{cpc}_{0}\mathrm{D}^{\varsigma}_{t}\mathbf{A}. \tag{56}$$

We have

$$\begin{aligned}{}^{cpc}\mathrm{D}^{\varsigma}_{t}\mathrm{M}(t) \leq\; & (\frac{\mathbf{X}-\mathbf{X}^{0}}{\mathbf{X}})\{\Lambda+(1-\rho)\beta_a\mathbf{A}\mathbf{I}_s+(1-q)\sigma\mathbf{I}_r-\beta\mathbf{X}\mathbf{I}_s-(1-c)\beta\mathbf{X}\mathbf{I}_r-\mu\mathbf{X}\}+\beta\mathbf{X}\mathbf{I}_s+q\sigma\mathbf{I}_r\\ & -\beta_a\mathbf{A}\mathbf{I}_s-(\delta_s+\mu)\mathbf{I}_s+(1-c)\beta\mathbf{X}\mathbf{I}_r+\rho\beta_a\mathbf{A}\mathbf{I}_s-(\delta_r+\sigma+\mu)\mathbf{I}_r+\alpha_s\mathbf{I}_s+\alpha_r\mathbf{I}_r-\mu_a\mathbf{A}.\end{aligned} \tag{57}$$

Putting $\mathbf{X}=\mathbf{X}-\mathbf{X}^0$, $\mathbf{I}_s=\mathbf{I}_s-\mathbf{I}_s^0$, $\mathbf{I}_r=\mathbf{I}_r-\mathbf{I}_r^0$, and $\mathbf{A}=\mathbf{A}-\mathbf{A}^0$ yields

$$\begin{aligned}{}^{cpc}\mathrm{D}^{\varsigma}_{t}\mathrm{M} \leq\; & (\frac{\mathbf{X}-\mathbf{X}^{0}}{\mathbf{X}})\{\Lambda+(1-\rho)\beta_a(\mathbf{A}-\mathbf{A}^0)(\mathbf{I}_s-\mathbf{I}_s^0)+(1-q)\sigma(\mathbf{I}_r-\mathbf{I}_r^0)-\beta(\mathbf{X}-\mathbf{X}^0)(\mathbf{I}_s-\mathbf{I}_s^0)\\ & -(1-c)\beta(\mathbf{X}-\mathbf{X}^0)(\mathbf{I}_r-\mathbf{I}_r^0)-\mu(\mathbf{X}-\mathbf{X}^0)\}+\beta(\mathbf{X}-\mathbf{X}^0)(\mathbf{I}_s-\mathbf{I}_s^0)+q\sigma(\mathbf{I}_r-\mathbf{I}_r^0)\\ & -\beta_a(\mathbf{A}-\mathbf{A}^0)(\mathbf{I}_s-\mathbf{I}_s^0)-(\delta_s+\mu)(\mathbf{I}_s-\mathbf{I}_s^0)+(1-c)\beta(\mathbf{X}-\mathbf{X}^0)(\mathbf{I}_r-\mathbf{I}_r^0)+\rho\beta_a(\mathbf{A}-\mathbf{A}^0)(\mathbf{I}_s-\mathbf{I}_s^0)\\ & -(\delta_r+\sigma+\mu)(\mathbf{I}_r-\mathbf{I}_r^0)+\alpha_s(\mathbf{I}_s-\mathbf{I}_s^0)+\alpha_r(\mathbf{I}_r-\mathbf{I}_r^0)-\mu_a(\mathbf{A}-\mathbf{A}^0),\\ \leq\; & -\Lambda\frac{\mathbf{X}^0}{\mathbf{X}}+(\frac{\mathbf{X}-\mathbf{X}^{0}}{\mathbf{X}})\{(1-\rho)\beta_a(\mathbf{A}-\mathbf{A}^0)(\mathbf{I}_s-\mathbf{I}_s^0)+(1-q)\sigma(\mathbf{I}_r-\mathbf{I}_r^0)-\beta(\mathbf{X}-\mathbf{X}^0)(\mathbf{I}_s-\mathbf{I}_s^0)\\ & -(1-c)\beta(\mathbf{X}-\mathbf{X}^0)(\mathbf{I}_r-\mathbf{I}_r^0)-\mu(\mathbf{X}-\mathbf{X}^0)\}+\beta(\mathbf{X}-\mathbf{X}^0)(\mathbf{I}_s-\mathbf{I}_s^0)+q\sigma(\mathbf{I}_r-\mathbf{I}_r^0)\\ & -\beta_a(\mathbf{A}-\mathbf{A}^0)(\mathbf{I}_s-\mathbf{I}_s^0)-(\delta_s+\mu)(\mathbf{I}_s-\mathbf{I}_s^0)+(1-c)\beta(\mathbf{X}-\mathbf{X}^0)(\mathbf{I}_r-\mathbf{I}_r^0)+\rho\beta_a(\mathbf{A}-\mathbf{A}^0)(\mathbf{I}_s-\mathbf{I}_s^0)\\ & -(\delta_r+\sigma+\mu)(\mathbf{I}_r-\mathbf{I}_r^0)+\alpha_s(\mathbf{I}_s-\mathbf{I}_s^0)+\alpha_r(\mathbf{I}_r-\mathbf{I}_r^0)-\mu_a(\mathbf{A}-\mathbf{A}^0).\end{aligned} \tag{58}$$

We observe that ${}^{cpc}\mathrm{D}^{\varsigma}_{t}\mathrm{M} \leq 0$ for $\mathrm{R}_{\mathrm{I}_s}, \mathrm{R}_{\mathrm{I}_r} < 1$, and ${}^{cpc}\mathrm{D}^{\varsigma}_{t}\mathrm{M} = 0$ iff $\mathbf{X}=\mathbf{X}^0$, $\mathbf{I}_s=\mathbf{I}_s^0$, $\mathbf{I}_r=\mathbf{I}_r^0$, and $\mathbf{A}=\mathbf{A}^0$. The bacteria-free equilibrium is thus a globally asymptotically stable point.

Theorem 4. *If* $\mathrm{R}_{\mathrm{I}_s} > 1$ *and* $\mathrm{R}_{\mathrm{I}_r} > 1$, *the endemic equilibrium point, denoted by* $(P_2,\ P_3,\ P_4)$, *of the fractional-order system (7) is globally asymptotically stable.*

Proof. We define the Lyapunov function as

$$\begin{aligned} \mathrm{M}(t) \ &= \ j_1(\mathbf{X}-\mathbf{X}^\bullet-\mathbf{X}^\bullet\ln\frac{\mathbf{X}}{\mathbf{X}^\bullet}) \ + \ j_2(\mathbf{I}_s-\mathbf{I}_s^\bullet-\mathbf{I}_s^\bullet\ln\frac{\mathbf{I}_s}{\mathbf{I}_s^\bullet}), \\ &+ \ j_3(\mathbf{I}_r-\mathbf{I}_r^\bullet-\mathbf{I}_r^\bullet\ln\frac{\mathbf{I}_r}{\mathbf{I}_r^\bullet}) \ + \ j_4(\mathbf{A}-\mathbf{A}^\bullet-\mathbf{A}^\bullet\ln\frac{\mathbf{A}}{\mathbf{A}^\bullet}) \end{aligned} \tag{59}$$

where $j_1, j_2, j_3, j_4, j_5, j_6$ are arbitrary positive constants. Equation (59) is then substituted into the system (7) to get

$${}^{cpc}\mathrm{D}_t^{\varsigma}\mathrm{M}(t) \ \leq \ j_1(\frac{\mathbf{X}-\mathbf{X}^\bullet}{\mathbf{X}})\,{}_0^{cpc}\mathrm{D}_t^{\varsigma}\mathbf{X} \ + \ j_2(\frac{\mathbf{I}_s-\mathbf{I}_s^\bullet}{\mathbf{I}_s})\,{}_0^{cpc}\mathrm{D}_t^{\varsigma}\mathbf{I}_s \ + \ j_3(\frac{\mathbf{I}_r-\mathbf{I}_r^\bullet}{\mathbf{I}_r})\,{}_0^{cpc}\mathrm{D}_t^{\varsigma}\mathbf{I}_r \ + \ j_4(\frac{\mathbf{A}-\mathbf{A}^\bullet}{\mathbf{A}})\,{}_0^{cpc}\mathrm{D}_t^{\varsigma}\mathbf{A}. \tag{60}$$

We have

$$\begin{aligned} {}^{cpc}\mathrm{D}_t^{\varsigma}\mathrm{M}(t) \ &\leq \ j_1(\frac{\mathbf{X}-\mathbf{X}^\bullet}{\mathbf{X}})\{\Lambda+(1-\rho)\beta_a\mathbf{A}\mathbf{I}_s+(1-q)\sigma\mathbf{I}_r-\beta\mathbf{X}\mathbf{I}_s-(1-c)\beta\mathbf{X}\mathbf{I}_r-\mu\mathbf{X}\} \\ &+ \ j_2(\frac{\mathbf{I}_s-\mathbf{I}_s^\bullet}{\mathbf{I}_s})\{\beta\mathbf{X}\mathbf{I}_s+q\sigma\mathbf{I}_r-\beta_a\mathbf{A}\mathbf{I}_s-(\delta_s+\mu)\mathbf{I}_s\} \\ &+ \ j_3(\frac{\mathbf{I}_r-\mathbf{I}_r^\bullet}{\mathbf{I}_r})\{(1-c)\beta\mathbf{X}\mathbf{I}_r+\rho\beta_a\mathbf{A}\mathbf{I}_s-(\delta_r+\sigma+\mu)\mathbf{I}_r\} \\ &+ \ j_4(\frac{\mathbf{A}-\mathbf{A}^\bullet}{\mathbf{A}})\{\alpha_s\mathbf{I}_s+\alpha_r\mathbf{I}_r-\mu_a\mathbf{A}\}. \end{aligned} \tag{61}$$

Putting $\mathbf{X}=\mathbf{X}-\mathbf{X}^\bullet$, $\mathbf{I}_s=\mathbf{I}_s-\mathbf{I}_s^\bullet$, $\mathbf{I}_r=\mathbf{I}_r-\mathbf{I}_r^\bullet$, and $\mathbf{A}=\mathbf{A}-\mathbf{A}^\bullet$ yields

$$\begin{aligned} {}^{cpc}\mathrm{D}_t^{\varsigma}\mathrm{M}(t) \ &\leq \ j_1(\frac{\mathbf{X}-\mathbf{X}^\bullet}{\mathbf{X}})\{\Lambda+(1-\rho)\beta_a(\mathbf{A}-\mathbf{A}^\bullet)(\mathbf{I}_s-\mathbf{I}_s^\bullet)+(1-q)\sigma(\mathbf{I}_r-\mathbf{I}_r^\bullet)-\beta(\mathbf{X}-\mathbf{X}^\bullet)(\mathbf{I}_s-\mathbf{I}_s^\bullet) \\ &\quad -(1-c)\beta(\mathbf{X}-\mathbf{X}^\bullet)(\mathbf{I}_r-\mathbf{I}_r^\bullet)-\mu(\mathbf{X}-\mathbf{X}^\bullet)\} \\ &+ j_2(\frac{\mathbf{I}_s-\mathbf{I}_s^\bullet}{\mathbf{I}_s})\{\beta(\mathbf{X}-\mathbf{X}^\bullet)(\mathbf{I}_s-\mathbf{I}_s^\bullet)+q\sigma(\mathbf{I}_r-\mathbf{I}_r^\bullet)-\beta_a(\mathbf{A}-\mathbf{A}^\bullet)(\mathbf{I}_s-\mathbf{I}_s^\bullet)-(\delta_s+\mu)(\mathbf{I}_s-\mathbf{I}_s^\bullet)\} \\ &+ \ j_3(\frac{\mathbf{I}_r-\mathbf{I}_r^\bullet}{\mathbf{I}_r})\{(1-c)\beta(\mathbf{X}-\mathbf{X}^\bullet)(\mathbf{I}_r-\mathbf{I}_r^\bullet)+\rho\beta_a(\mathbf{A}-\mathbf{A}^\bullet)(\mathbf{I}_s-\mathbf{I}_s^\bullet)-(\delta_r+\sigma+\mu)(\mathbf{I}_r-\mathbf{I}_r^\bullet)\} \\ &+ \ j_4(\frac{\mathbf{A}-\mathbf{A}^\bullet}{\mathbf{A}})\{\alpha_s(\mathbf{I}_s-\mathbf{I}_s^\bullet)+\alpha_r(\mathbf{I}_r-\mathbf{I}_r^\bullet)-\mu_a(\mathbf{A}-\mathbf{A}^\bullet)\}. \end{aligned} \tag{62}$$

$$
\begin{aligned}
{}^{cpc}\mathrm{D}_t^{\varsigma}\mathrm{M}(t) \;\leq\; & j_1\Lambda - j_1\Lambda\frac{\mathbf{X}^{\bullet}}{\mathbf{X}} + j_1(1-\rho)\beta_a(\mathbf{A}-\mathbf{A}^{\bullet})(\mathbf{I}_s-\mathbf{I}_s^{\bullet}) - j_1(1-\rho)\beta_a(\mathbf{A}-\mathbf{A}^{\bullet})\frac{\mathbf{X}^{\bullet}}{\mathbf{X}}(\mathbf{I}_s-\mathbf{I}_s^{\bullet}) \\
& + j_1(1-q)\sigma(\mathbf{I}_r-\mathbf{I}_r^{\bullet}) - j_1(1-q)\sigma\frac{\mathbf{X}^{\bullet}}{\mathbf{X}}(\mathbf{I}_r-\mathbf{I}_r^{\bullet}) - j_1\beta\frac{(\mathbf{X}-\mathbf{X}^{\bullet})^2}{\mathbf{X}}(\mathbf{I}_s-\mathbf{I}_s^{\bullet}) \\
& - j_1(1-c)\beta(\mathbf{X}-\mathbf{X}^{\bullet})(\mathbf{I}_r-\mathbf{I}_r^{\bullet}) - j_1\mu(\mathbf{X}-\mathbf{X}^{\bullet}) + j_2\beta(\mathbf{X}-\mathbf{X}^{\bullet})\frac{(\mathbf{I}_s-\mathbf{I}_s^{\bullet})^2}{\mathbf{I}_s} + j_2q\sigma(\mathbf{I}_r-\mathbf{I}_r^{\bullet}) \\
& - j_2q\sigma(\mathbf{I}_r-\mathbf{I}_r^{\bullet})\frac{\mathbf{I}_s^{\bullet}}{\mathbf{I}_s} - j_2\beta_a(\mathbf{A}-\mathbf{A}^{\bullet})\frac{(\mathbf{I}_s-\mathbf{I}_s^{\bullet})^2}{\mathbf{I}_s} - j_2(\delta_s+\mu)\frac{(\mathbf{I}_s-\mathbf{I}_s^{\bullet})^2}{\mathbf{I}_s} \\
& + \; j_3(1-c)\beta(\mathbf{X}-\mathbf{X}^{\bullet})\frac{(\mathbf{I}_r-\mathbf{I}_r^{\bullet})^2}{\mathbf{I}_r} + j_3\rho\beta_a(\mathbf{A}-\mathbf{A}^{\bullet})(\mathbf{I}_s-\mathbf{I}_s^{\bullet}) - j_3\rho\beta_a(\mathbf{A}-\mathbf{A}^{\bullet})\frac{(\mathbf{I}_r^{\bullet})^2}{\mathbf{I}_r}(\mathbf{I}_s-\mathbf{I}_s^{\bullet}) \\
& - \; j_3(\delta_r+\sigma+\mu)\frac{(\mathbf{I}_r-\mathbf{I}_r^{\bullet})^2}{\mathbf{I}_r} + j_4\alpha_s(\mathbf{I}_s-\mathbf{I}_s^{\bullet}) - j_4\alpha_s(\mathbf{I}_s-\mathbf{I}_s^{\bullet})\frac{(\mathbf{A}^{\bullet})^2}{\mathbf{A}} + j_4\alpha_r(\mathbf{I}_r-\mathbf{I}_r^{\bullet}) \\
& - \; j_4\alpha_r(\mathbf{I}_r-\mathbf{I}_r^{\bullet})\frac{(\mathbf{A}^{\bullet})^2}{\mathbf{A}} - j_4\mu_a\frac{(\mathbf{A}-\mathbf{A}^{\bullet})^2}{\mathbf{A}}.
\end{aligned}
\tag{63}
$$

Now, let $j_1 = j_2 = j_3 = j_4 = 1$, and finally we have

$$
{}_0^{cpc}\mathrm{D}_t^{\varsigma}\mathrm{M}(t) = \delta_1 - \delta_2, \tag{64}
$$

where

$$
\begin{aligned}
\delta_1 =& \Lambda + (1-\rho)\beta_a(\mathbf{A}-\mathbf{A}^{\bullet})(\mathbf{I}_s-\mathbf{I}_s^{\bullet}) + (1-q)\sigma(\mathbf{I}_r-\mathbf{I}_r^{\bullet}) + \beta(\mathbf{X}-\mathbf{X}^{\bullet})\frac{(\mathbf{I}_s-\mathbf{I}_s^{\bullet})^2}{\mathbf{I}_s} + q\sigma(\mathbf{I}_r-\mathbf{I}_r^{\bullet}) \\
& + (1-c)\beta(\mathbf{X}-\mathbf{X}^{\bullet})\frac{(\mathbf{I}_r-\mathbf{I}_r^{\bullet})^2}{\mathbf{I}_r} + \rho\beta_a(\mathbf{A}-\mathbf{A}^{\bullet})(\mathbf{I}_s-\mathbf{I}_s^{\bullet}) + \alpha_s(\mathbf{I}_s-\mathbf{I}_s^{\bullet}) + \alpha_r(\mathbf{I}_r-\mathbf{I}_r^{\bullet}).
\end{aligned}
\tag{65}
$$

and

$$
\begin{aligned}
\delta_2 =& \Lambda\frac{\mathbf{X}^{\bullet}}{\mathbf{X}} + (1-\rho)\beta_a(\mathbf{A}-\mathbf{A}^{\bullet})\frac{\mathbf{X}^{\bullet}}{\mathbf{X}}(\mathbf{I}_s-\mathbf{I}_s^{\bullet}) + (1-q)\sigma\frac{\mathbf{X}^{\bullet}}{\mathbf{X}}(\mathbf{I}_r-\mathbf{I}_r^{\bullet}) + \beta\frac{(\mathbf{X}-\mathbf{X}^{\bullet})^2}{\mathbf{X}}(\mathbf{I}_s-\mathbf{I}_s^{\bullet}) \\
& + (1-c)\beta(\mathbf{X}-\mathbf{X}^{\bullet})(\mathbf{I}_r-\mathbf{I}_r^{\bullet}) + \mu(\mathbf{X}-\mathbf{X}^{\bullet}) + q\sigma(\mathbf{I}_r-\mathbf{I}_r^{\bullet})\frac{\mathbf{I}_s^{\bullet}}{\mathbf{I}_s} + \beta_a(\mathbf{A}-\mathbf{A}^{\bullet})\frac{(\mathbf{I}_s-\mathbf{I}_s^{\bullet})^2}{\mathbf{I}_s} \\
& + (\delta_s+\mu)\frac{(\mathbf{I}_s-\mathbf{I}_s^{\bullet})^2}{\mathbf{I}_s} + \rho\beta_a(\mathbf{A}-\mathbf{A}^{\bullet})\frac{(\mathbf{I}_r^{\bullet})^2}{\mathbf{I}_r}(\mathbf{I}_s-\mathbf{I}_s^{\bullet}) + (\delta_r+\sigma+\mu)\frac{(\mathbf{I}_r-\mathbf{I}_r^{\bullet})^2}{\mathbf{I}_r} + \alpha_s(\mathbf{I}_s-\mathbf{I}_s^{\bullet})\frac{(\mathbf{A}^{\bullet})^2}{\mathbf{A}} \\
& + \alpha_r(\mathbf{I}_r-\mathbf{I}_r^{\bullet})\frac{(\mathbf{A}^{\bullet})^2}{\mathbf{A}} + \mu_a\frac{(\mathbf{A}-\mathbf{A}^{\bullet})^2}{\mathbf{A}}.
\end{aligned}
\tag{66}
$$

From Equation (64), we observe that

- ${}_0^{cpc}D_t^{\varsigma}\mathrm{M} \leq 0$ for $\mathscr{R}_0 > 1$, and
- ${}_0^{cpc}D_t^{\varsigma}\mathrm{M} = 0$ for $\mathbf{X} = \mathbf{X}^{\bullet},\ \mathbf{I}_s = \mathbf{I}_s^{\bullet},\ \mathbf{I}_r = \mathbf{I}_r^{\bullet},\ \mathbf{A} = \mathbf{A} - \mathbf{A}^{\bullet}$.

It suggests that our proposed system (7) is globally asymptotically stable globally.

5.6. Chaos Control

The linear feedback regulate method is used to stabilize system (7) based on its locations of equilibrium, taking into consideration a fractional-order system with a controlled design.

$$\begin{cases} {}^{cpc}{}_0D_t^{\varsigma}\mathbf{X}(t) &= \Lambda+(1-\rho)\beta_a\mathbf{A}\mathbf{I}_s+(1-q)\sigma\mathbf{I}_r-\beta\mathbf{X}\mathbf{I}_s-(1-c)\beta\mathbf{X}\mathbf{I}_r-\mu\mathbf{X}-\varpi_1(\mathbf{X}-\mathbf{X}^*),\\ {}^{cpc}{}_0D_t^{\varsigma}\mathbf{I}_s(t) &= \beta\mathbf{X}\mathbf{I}_s+q\sigma\mathbf{I}_r-\beta_a\mathbf{A}\mathbf{I}_s-(\delta_s+\mu)\mathbf{I}_s-\varpi_2(\mathbf{I}_s-\mathbf{I}_s^*),\\ {}^{cpc}{}_0D_t^{\varsigma}\mathbf{I}_r(t) &= (1-c)\beta\mathbf{X}\mathbf{I}_r+\rho\beta_a\mathbf{A}\mathbf{I}_s-(\delta_r+\sigma+\mu)\mathbf{I}_r-\varpi_3(\mathbf{I}_r-\mathbf{I}_r^*),\\ {}^{cpc}{}_0D_t^{\varsigma}\mathbf{A}(t) &= \alpha_s\mathbf{I}_s+\alpha_r\mathbf{I}_r-\mu_a\mathbf{A}-\varpi_4(\mathbf{A}-\mathbf{A}^*). \end{cases} \tag{67}$$

where control parameters are expressed by ϖ_1, ϖ_2,, ϖ_3, and ϖ_4, while $\{\Theta^*\}$ shows the proposed system (7)'s equilibrium points. The Jacobian matrix at $\{\Theta^*\}$ is given by

$$J(\Theta^*)=\begin{bmatrix} -\mu-\varpi_1 & -\frac{\beta\Lambda}{\mu} & -q\sigma-c\frac{\beta\Lambda}{\mu} & 0\\ 0 & \frac{\beta\Lambda}{\mu}-(\delta_s+\mu)-\varpi_2 & 0 & 0\\ 0 & 0 & -c\frac{\beta\Lambda}{\mu}-(\delta_r+\sigma+\mu)-\varpi_3 & 0\\ 0 & \alpha_s & \alpha_r & -\mu_a-\varpi_4 \end{bmatrix}. \tag{68}$$

We find the characteristic equation as follows:

$$f(\varphi)=\begin{bmatrix} \varphi+\mu+\varpi_1 & -\frac{\beta\Lambda}{\mu} & -q\sigma-c\frac{\beta\Lambda}{\mu} & 0\\ 0 & \varphi-\frac{\beta\Lambda}{\mu}+(\delta_s+\mu)+\varpi_2 & 0 & 0\\ 0 & 0 & \varphi+c\frac{\beta\Lambda}{\mu}+(\delta_r+\sigma+\mu)+\varpi_3 & 0\\ 0 & \alpha_s & \alpha_r & \varphi+\mu_a+\varpi_4 \end{bmatrix}. \tag{69}$$

Now, suppose that $\varpi_1=1$, $\varpi_2=2$, $\varpi_3=3$, and $\varpi_4=4$, then we get

$$\begin{aligned} &\varphi_1=-\mu-1, \qquad \varphi_2=-(\delta_s+\mu)+\frac{\beta\Lambda}{\mu}-2,\\ &\varphi_3=-c\frac{\beta\Lambda}{\mu}-(\delta_r+\sigma+\mu)-3, \qquad \varphi_4=-\mu_a-. \end{aligned} \tag{70}$$

The equilibrium points exhibit asymptotic stability since each eigenvalue is negative.

6. Numerical Scheme

Following from Theorem (1) and using Laplace transform, we have

$$\begin{cases} [\frac{\mathrm{V}_1(\varsigma)}{r}+\mathrm{V}_0(\varsigma)]r^{\varsigma}\bar{\mathbf{X}}(r)-\mathrm{V}_0(\varsigma)r^{\varsigma-1}\mathbf{X}_0=\mathscr{L}[\Lambda+(1-\rho)\beta_a\mathbf{A}\mathbf{I}_s+(1-q)\sigma\mathbf{I}_r-\beta\mathbf{X}\mathbf{I}_s-(1-c)\beta\mathbf{X}\mathbf{I}_r-\mu\mathbf{X}],\\ [\frac{\mathrm{V}_1(\varsigma)}{r}+\mathrm{V}_0(\varsigma)]r^{\varsigma}\bar{\mathbf{I}}_s(r)-\mathrm{V}_0(\varsigma)r^{\varsigma-1}\mathbf{I}_{s_0}=\mathscr{L}[\beta\mathbf{X}\mathbf{I}_s+q\sigma\mathbf{I}_r-\beta_a\mathbf{A}\mathbf{I}_s-(\delta_s+\mu)\mathbf{I}_s],\\ [\frac{\mathrm{V}_1(\varsigma)}{r}+\mathrm{V}_0(\varsigma)]r^{\varsigma}\bar{\mathbf{I}}_r(r)-\mathrm{V}_0(\varsigma)r^{\varsigma-1}\mathbf{I}_{s_0}=\mathscr{L}[(1-c)\beta\mathbf{X}\mathbf{I}_r+\rho\beta_a\mathbf{A}\mathbf{I}_s-(\delta_r+\sigma+\mu)\mathbf{I}_r],\\ [\frac{\mathrm{V}_1(\varsigma)}{r}+\mathrm{V}_0(\varsigma)]r^{\varsigma}\bar{\mathbf{A}}(r)-\mathrm{V}_0(\varsigma)r^{\varsigma-1}\mathbf{X}_0=\mathscr{L}[\alpha_s\mathbf{I}_s+\alpha_r\mathbf{I}_r-\mu_a\mathbf{A}]. \end{cases} \tag{71}$$

where

$$\mathscr{L}(\mathbf{X}(t))=\bar{\mathbf{X}}(r),\ \ \mathscr{L}(\mathbf{I}_s(t))=\bar{\mathbf{I}}_s(r),\ \ \mathscr{L}(\mathbf{I}_r(t))=\bar{\mathbf{I}}_r(r),\ \ \mathscr{L}(\mathbf{A}(t))=\bar{\mathbf{A}}(r). \tag{72}$$

Furthermore, we can write

$$\begin{aligned}
\mathscr{L}(\mathbf{X}(t)) &= \frac{\mathbf{X}_0}{r+\frac{\mathrm{V}_1(\varsigma)}{\mathrm{V}_0(\varsigma)}}+\left(\mathrm{V}_0(\varsigma)\left[1+\frac{\mathrm{V}_1(\varsigma)}{\mathrm{V}_0(\varsigma)}r^{-1}\right]r^{\varsigma}\right)^{-1}\\
&\quad\times\mathscr{L}[\Lambda+(1-\rho)\beta_a\mathbf{A}\mathbf{I}_s+(1-q)\sigma\mathbf{I}_r-\beta\mathbf{X}\mathbf{I}_s-(1-c)\beta\mathbf{X}\mathbf{I}_r-\mu\mathbf{X}],\\
\mathscr{L}(\mathbf{I}_s(t)) &= \frac{\mathbf{I}_{s_0}}{r+\frac{\mathrm{V}_1(\varsigma)}{\mathrm{V}_0(\varsigma)}}+\left(\mathrm{V}_0(\varsigma)\left[1+\frac{\mathrm{V}_1(\varsigma)}{\mathrm{V}_0(\varsigma)}r^{-1}\right]r^{\varsigma}\right)^{-1}\times\mathscr{L}[\beta\mathbf{X}\mathbf{I}_s+q\sigma\mathbf{I}_r-\beta_a\mathbf{A}\mathbf{I}_s-(\delta_s+\mu)\mathbf{I}_s],\\
\mathscr{L}(\mathbf{I}_r(t)) &= \frac{\mathbf{I}_{r_0}}{r+\frac{\mathrm{V}_1(\varsigma)}{\mathrm{V}_0(\varsigma)}}+\left(\mathrm{V}_0(\varsigma)\left[1+\frac{\mathrm{V}_1(\varsigma)}{\mathrm{V}_0(\varsigma)}r^{-1}\right]r^{\varsigma}\right)^{-1}\times\mathscr{L}[(1-c)\beta\mathbf{X}\mathbf{I}_r+\rho\beta_a\mathbf{A}\mathbf{I}_s-(\delta_r+\sigma+\mu)\mathbf{I}_r],\\
\mathscr{L}(\mathbf{A}(t)) &= \frac{\mathbf{X}_0}{r+\frac{\mathrm{V}_1(\varsigma)}{\mathrm{V}_0(\varsigma)}}+\left(\mathrm{V}_0(\varsigma)\left[1+\frac{\mathrm{V}_1(\varsigma)}{\mathrm{V}_0(\varsigma)}r^{-1}\right]r^{\varsigma}\right)^{-1}\times\mathscr{L}[\alpha_s\mathbf{I}_s+\alpha_r\mathbf{I}_r-\mu_a\mathbf{A}].
\end{aligned}\tag{73}$$

This can be written as

$$\begin{aligned}
\mathscr{L}(\mathbf{X}(t)) &= \frac{\mathbf{X}_0}{r+\frac{\mathrm{V}_1(\varsigma)}{\mathrm{V}_0(\varsigma)}}+\sum_{q=0}^{\infty}\frac{-(\mathrm{V}_1(\varsigma))^q}{(\mathrm{V}_0(\varsigma))^{q+1}}r^{-\varsigma-q}\\
&\quad\times\mathscr{L}[\Lambda+(1-\rho)\beta_a\mathbf{A}\mathbf{I}_s+(1-q)\sigma\mathbf{I}_r-\beta\mathbf{X}\mathbf{I}_s-(1-c)\beta\mathbf{X}\mathbf{I}_r-\mu\mathbf{X}],\\
\mathscr{L}(\mathbf{I}_s(t)) &= \frac{\mathbf{I}_{s_0}}{r+\frac{\mathrm{V}_1(\varsigma)}{\mathrm{V}_0(\varsigma)}}+\sum_{q=0}^{\infty}\frac{-(\mathrm{V}_1(\varsigma))^q}{(\mathrm{V}_0(\varsigma))^{q+1}}r^{-\varsigma-q}\times\mathscr{L}[\beta\mathbf{X}\mathbf{I}_s+q\sigma\mathbf{I}_r-\beta_a\mathbf{A}\mathbf{I}_s-(\delta_s+\mu)\mathbf{I}_s],\\
\mathscr{L}(\mathbf{I}_r(t)) &= \frac{\mathbf{I}_{r_0}}{r+\frac{\mathrm{V}_1(\varsigma)}{\mathrm{V}_0(\varsigma)}}+\sum_{q=0}^{\infty}\frac{-(\mathrm{V}_1(\varsigma))^q}{(\mathrm{V}_0(\varsigma))^{q+1}}r^{-\varsigma-q}\times\mathscr{L}[(1-c)\beta\mathbf{X}\mathbf{I}_r+\rho\beta_a\mathbf{A}\mathbf{I}_s-(\delta_r+\sigma+\mu)\mathbf{I}_r],\\
\mathscr{L}(\mathbf{A}(t)) &= \frac{\mathbf{A}_0}{r+\frac{\mathrm{V}_1(\varsigma)}{\mathrm{V}_0(\varsigma)}}+\sum_{q=0}^{\infty}\frac{-(\mathrm{V}_1(\varsigma))^q}{(\mathrm{V}_0(\varsigma))^{q+1}}r^{-\varsigma-q}\times\mathscr{L}[\alpha_s\mathbf{I}_s+\alpha_r\mathbf{I}_r-\mu_a\mathbf{A}].
\end{aligned}\tag{74}$$

We assume that solution obtained by the method should be expressed as an infinite series as follows:

$$\mathbf{X}(t)=\sum_{j=0}^{\infty}\mathbf{X}_j,\ \ \mathbf{I_s}(t)=\sum_{j=0}^{\infty}\mathbf{I_s}_j,\ \ \mathbf{I_r}(t)=\sum_{j=0}^{\infty}\mathbf{I_r}_j,\ \ \mathbf{A}(t)=\sum_{j=0}^{\infty}\mathbf{A}_j, \tag{75}$$

where the product terms $\mathbf{AI}_s$, $\mathbf{XI_s}$, and $\mathbf{XI_r}$ can be expressed in the following manner:

$$\begin{aligned}
\mathbf{AI}_s &= \sum_{j=0}^{\infty}\mathscr{A}_j(t),\quad \mathscr{A}_j=\frac{1}{j!}\left(\frac{d}{d\varsigma}\right)^j\left[\sum_{p=0}^{j}\varsigma^p\mathbf{A}_p\sum_{p=0}^{j}\varsigma^p\mathbf{I_s}_p\right]_{\varsigma=0},\\
\mathbf{XI}_s &= \sum_{j=0}^{\infty}\mathscr{B}_j(t),\quad \mathscr{B}_j=\frac{1}{j!}\left(\frac{d}{d\varsigma}\right)^j\left[\sum_{p=0}^{j}\varsigma^p\mathbf{X}_p\sum_{p=0}^{j}\varsigma^p\mathbf{I_s}_p\right]_{\varsigma=0},
\end{aligned}\tag{76}$$

$$\mathbf{XI}_r \;=\; \sum_{j=0}^{\infty}\mathscr{C}_j(t), \quad \mathscr{C}_j \;=\; \frac{1}{j!}\left(\frac{d}{d\varsigma}\right)^j\left[\sum_{p=0}^{j}\varsigma^p\mathbf{X}_p\sum_{p=0}^{j}\varsigma^p\mathbf{I_r}_p\right]_{\varsigma=0},$$

where $j = 1,2,3,\cdots$.
After some calculations, we get finally the following iterative solutions

$$\begin{aligned}
\mathbf{X}_{k+1}(t) &= \mathbf{X}_0\exp\Big(\frac{-\mathrm{V}_1(\varsigma)}{\mathrm{V}_0(\varsigma)}t\Big)+\frac{1}{\mathrm{V}_0(\varsigma)}\sum_{j=0}^{\infty}\Big(\frac{-\mathrm{V}_1(\varsigma)}{\mathrm{V}_0(\varsigma)}\Big)^{j+1}\frac{t^{\varsigma+j-1}}{\Gamma(\varsigma+j)}\\
&\quad\times\mathscr{L}^{-1}\Big\{\mathscr{L}[\Lambda+(1-\rho)\beta_a\mathbf{AI}_s+(1-q)\sigma\mathbf{I}_r-\beta\mathbf{XI}_s-(1-c)\beta\mathbf{XI}_r-\mu\mathbf{X}]\Big\},\\
\mathbf{I_s}_{k+1}(t) &= \mathbf{I_{s_0}}\exp\Big(\frac{-\mathrm{V}_1(\varsigma)}{\mathrm{V}_0(\varsigma)}t\Big)+\frac{1}{\mathrm{V}_0(\varsigma)}\sum_{j=0}^{\infty}\Big(\frac{-\mathrm{V}_1(\varsigma)}{\mathrm{V}_0(\varsigma)}\Big)^{j+1}\frac{t^{\varsigma+j-1}}{\Gamma(\varsigma+j-1)}\\
&\quad\times\mathscr{L}^{-1}\Big\{\mathscr{L}[\beta\mathbf{XI}_s+q\sigma\mathbf{I}_r-\beta_a\mathbf{AI}_s-(\delta_s+\mu)\mathbf{I}_s]\Big\},\\
\mathbf{I_r}_{k+1}(t) &= \mathbf{I_{r_0}}\exp\Big(\frac{-\mathrm{V}_1(\varsigma)}{\mathrm{V}_0(\varsigma)}t\Big)+\frac{1}{\mathrm{V}_0(\varsigma)}\sum_{j=0}^{\infty}\Big(\frac{-\mathrm{V}_1(\varsigma)}{\mathrm{V}_0(\varsigma)}\Big)^{j+1}\frac{t^{\varsigma+j-1}}{\Gamma(\varsigma+j-1)}\\
&\quad\times\mathscr{L}^{-1}\Big\{\mathscr{L}[(1-c)\beta\mathbf{XI}_r+\rho\beta_a\mathbf{AI}_s-(\delta_r+\sigma+\mu)\mathbf{I}_r]\Big\},\\
\mathbf{A}_{k+1}(t) &= \mathbf{A}_0\exp\Big(\frac{-\mathrm{V}_1(\varsigma)}{\mathrm{V}_0(\varsigma)}t\Big)+\frac{1}{\mathrm{V}_0(\varsigma)}\sum_{j=0}^{\infty}\Big(\frac{-\mathrm{V}_1(\varsigma)}{\mathrm{V}_0(\varsigma)}\Big)^{j+1}\frac{t^{\varsigma+j-1}}{\Gamma(\varsigma+j-1)}\times\mathscr{L}^{-1}\Big\{\mathscr{L}[\alpha_s\mathbf{I}_s+\alpha_r\mathbf{I}_r-\mu_a\mathbf{A}]\Big\}.
\end{aligned} \tag{77}$$

7. Results and Discussion

The efficiency of the suggested model is verified by numerical simulations and the Laplace Adomian decomposition approach. The model is reduced at various fractional orders of ς using a constant-proportional Caputo operator. Collecting statistics on community-associated bacterial diseases is difficult due to factors such as insufficient information (not all cases seek medical attention), medical staff underreporting, testing challenges, and the need to separate such infections from those that are collected in hospitals. The parametric variables mentioned in Table (2) have been incorporated into the proposed model to produce results. While some of the parametric values are derived from source [36], some are assumed. $\mathbf{X}(0) = 1000000$, $\mathbf{I_s}(0) = 100$, $\mathbf{I_r}(0) = 0$, and $\mathbf{A}(0) = 5000$ are the initial values for the variables. Simulations over a wide range of fractional values $\varsigma = 0.95, 0.90, 0.85$ have been presented. Simulations are coded in Matlab. To ascertain the advantageous effects of parameter values, a large number of simulations are performed. Reducing fractional values in each compartment results in a stable posture. Based on their varied values, the most important fractional parameters are chosen, and their impact on the dynamical behavior of infectious classes is investigated. Figure (3) shows that the groups $\mathbf{X}$, $\mathbf{I_s}$, $\mathbf{I_r}$, and $\mathbf{A}$ provide reliable solutions when the fractional order is reduced. Figure (3)a shows how humans respond to antibiotic-resistant illnesses when the CPC operator is applied to several fractional values. It is noticeable that the fractional value of sensitive persons decreases over time. As shown in figures

(3)b and (3)c, susceptible humans become infected with bacteria after coming into touch with infected individuals.

Table 2: Interpretation of model parameters [36]

Symbol	**Value**	**Range**	**Symbol**	**Value**	**Range**
Λ	0.0077	0-0.1	β	0.00000045	0-1
β_a	0.000861897	0-1	c	0.7	0-1
ρ	0.8	0-1	q	0.3	0-1
σ	0.007819	$10^{-5}-1$	α_s	0.1	0-0.15
α_r	0.05	0-0.15	μ	0.0077	0-0.1
μ_a	0.075	0-0.15	δ_s	5×10^{-8}	0-0.001
δ_r	0.0089	0-0.1			

When compared to the traditional operator, the numerical approach based on the Laplace Adomain Decomposition technique produces better results for all classes using the Constant Proportional Caputo operator. Furthermore, Figure (4) shows the numerical simulation of the groups **X**, $\mathbf{I_s}$, $\mathbf{I_r}$, and **A** using the Caputo fractional operator. Also, we compared the results of both operators, and their numerical findings are shown in tables (3)-(6).

Figures (3)c illustrate that even little increases in fractional order lead to a considerable increase in contagious population behavior. We can reduce the infected population by decreasing the ς value with a fair ratio. The conventional integer order model solution at $\varsigma = 1$ enables the comparison of numerical simulation findings to integer-order outcomes. Curves with $\varsigma = 0.95, 0.90, 0.85, 0.80$ exhibit slower rise/fall over longer periods than classical models.

The comparison graphs between CPC and Caputo, as shown in Figure (5), reveal that CPC fractional derivative outperforms integer-order and Caputo fractional derivatives due to non-local and non-singular features. The CPC derivative's kernel properties can influence model outputs, with higher values indicating greater sensitivity to past events and more detailed memory effects. A higher CPC curve indicates a more pronounced fractional memory, affecting future infection rates. A higher CPC curve indicates a faster accumulation of infected individuals over time. The CPC derivative allows for a broader range of dynamic behaviors, including complex disease trajectories, which could lead to more severe or prolonged outbreaks in real-world scenarios compared to a Caputo-based model. In the future, both these operators can be compared using conventional error measures like as Mean Absolute Error (MAE), Root Mean Squared Error (RMSE), and R-squared, along with visual aids like residual plots. These metrics will reflect model accuracy indicating better performance. Residual plots will help identify error patterns and probable nonlinearity issues. This study increases our understanding of complex interactions and has practical implications for managing issues such as bacterial infections. By including long-range memory effects associated with the progression, incubation, and recovery of bacterial diseases, the fractional formulation improves on conventional integer-order models. This methodology estimates the important epidemiological rates β, β_a, α_s, and α_s while simultaneously enabling the fractional

memory order ς to be learned as a trainable parameter.

Surface plots and contour plots for every compartment at different fractional order values within the feasible domain are shown in Figure (6). Surface plots provide a three-dimensional depiction in which the z-axis shows the state of the compartment (e.g., population number or concentration) and the x and y axes are two variables (e.g., time and fractional order). It shows how each compartment's dynamics fluctuate with time and different fractional orders. Additionally, these surface plots are used to create contour plots. Every contour line connects x and y input points that produce the same output values, such as fractional orders and the same population at a given time. The steepness of the function is indicated by the distance between these lines; narrower lines imply a more gradual shift, while closely spaced lines indicate a quick change.

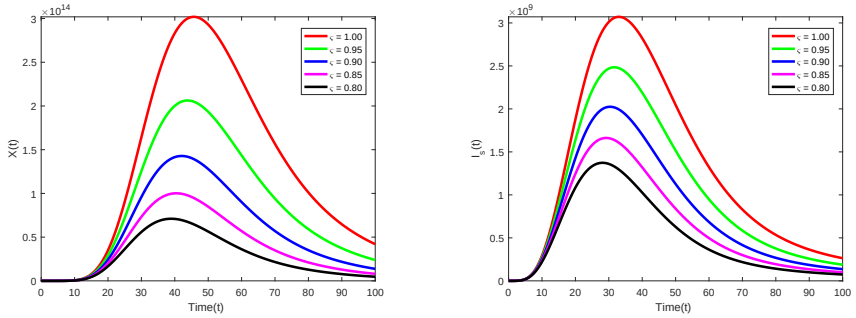

(a) **X**

(b) $\mathbf{I}_s$

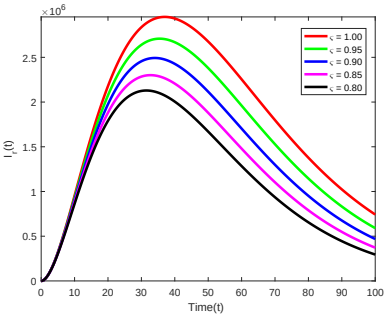

(c) $\mathbf{I}_r$

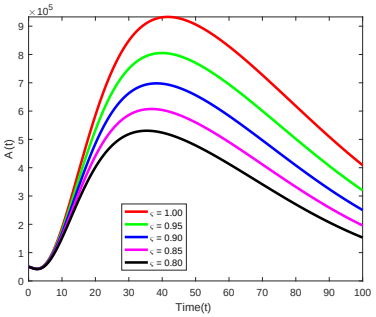

(d) **A**

Figure 3: Proposed model's simulations with CPC operator at various fractional values of ς

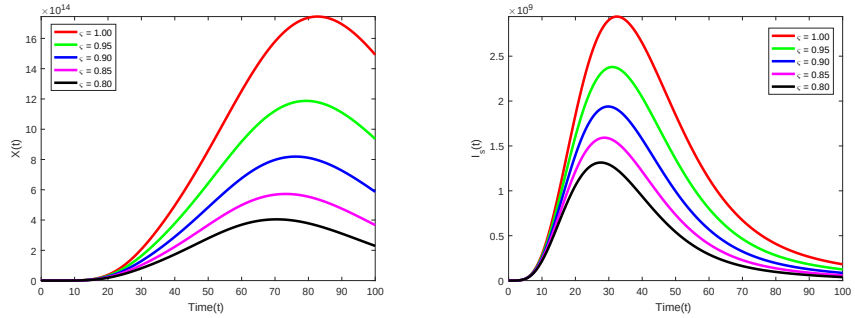

(a) **X** (b) $\mathbf{I}_s$

(c) $\mathbf{I}_r$ (d) **A**

Figure 4: Proposed model's simulations with Caputo operator at various fractional values of ς

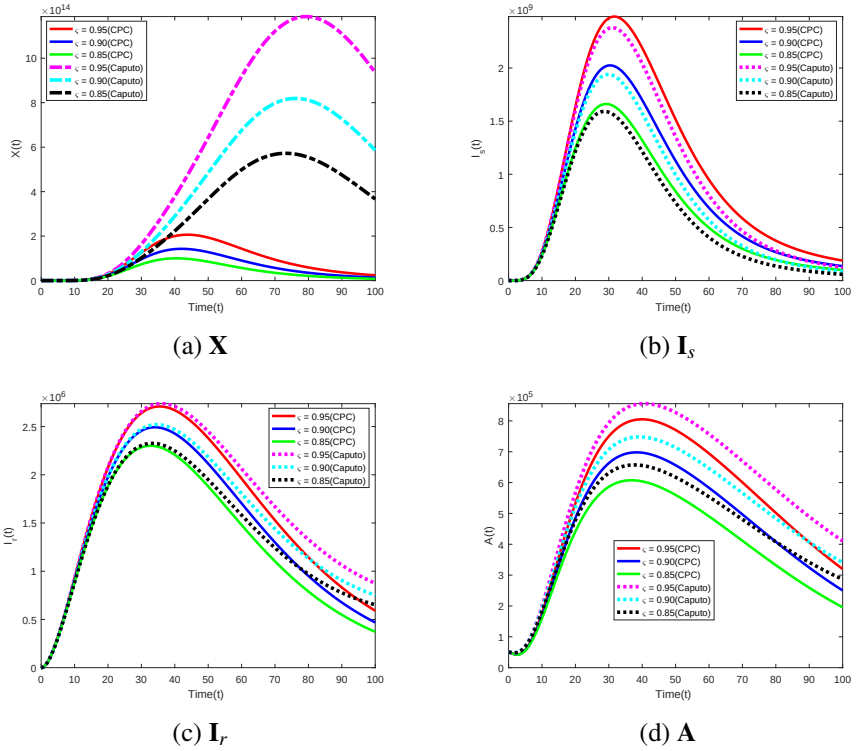

(a) **X** (b) $\mathbf{I}_s$

(c) $\mathbf{I}_r$ (d) **A**

Figure 5: Proposed model's simulations comparison between CPC and Caputo operators

Table 3: Numerical simulation of **X**

Time (months)	**CPC**			**Caputo**		
	$\varsigma = 0.95$	$\varsigma = 0.90$	$\varsigma = 0.85$	$\varsigma = 0.95$	$\varsigma = 0.90$	$\varsigma = 0.85$
0	1000000	1000000	1000000	1000000	1000000	1000000
10	5.438e+11	4.948e+11	4.501e+11	5.545e+11	5.053e+11	4.603e+11
20	2.906e+13	2.416e+13	2.008e+13	3.166e+13	2.657e+13	2.23e+13
30	1.255e+14	9.586e+13	7.320e+13	1.635e+14	1.292e+14	1.023e+14
40	2.002e+14	1.415e+14	1.001e+14	3.779e+14	2.896e+14	2.232e+14
50	1.933e+14	1.279e+14	8.479e+13	6.430e+14	4.844e+14	3.67e+14
60	1.435e+14	9.009e+13	5.691e+13	9.182e+14	6.755e+14	4.986e+14
70	9.400e+13	5.696e+13	3.485e+13	1.122e+15	7.977e+14	5.679e+14
80	5.913e+13	3.505e+13	2.104e+13	1.187e+15	8.111e+14	5.541e+14
90	3.727e+13	2.178e+13	1.289e+13	1.110e+15	7.267e+14	4.753e+14
100	2.383e+13	1.373e+13	8.002e+12	9.360e+14	5.864e+14	3.668e+14

Table 4: Numerical simulation of $\mathbf{I_s}$

Time (months)	**CPC**			**Caputo**		
	$\varsigma = 0.95$	$\varsigma = 0.90$	$\varsigma = 0.85$	$\varsigma = 0.95$	$\varsigma = 0.90$	$\varsigma = 0.85$
0	100	100	100	100	100	100
10	2.732e+08	2.546e+08	2.372e+08	2.711e+08	2.525e+08	2.351e+08
20	1.637e+09	1.428e+09	1.245e+09	1.605e+09	1.398e+09	1.217e+09
30	2.469e+09	2.024e+09	1.659e+09	2.373e+09	1.939e+09	1.548e+09
40	2.189e+09	1.699e+09	1.320e+09	2.041e+09	1.574e+09	1.215e+09
50	1.516e+09	1.127e+09	8.395e+08	1.354e+09	9.951e+08	7.330e+08
60	9.481e+08	6.841e+08	4.968e+08	8.012e+08	5.689e+08	4.061e+08
70	5.849e+08	4.166e+08	2.998e+08	4.648e+08	3.242e+08	2.281e+08
80	3.758e+08	2.679e+08	1.935e+08	2.809e+08	1.951e+08	1.367e+08
90	2.575e+08	1.85ee+08	1.348e+08	1.815e+08	1.259e+08	8.774e+07
100	1.880e+08	1.362e+08	9.995e+07	1.244e+08	8.534e+07	5.812e+07

Table 5: Numerical simulation of $\mathbf{I_r}$

Time (months)	**CPC**			**Caputo**		
	$\varsigma = 0.95$	$\varsigma = 0.90$	$\varsigma = 0.85$	$\varsigma = 0.95$	$\varsigma = 0.90$	$\varsigma = 0.85$
0	0	0	0	0	0	0
10	9.302e+05	9.071e+05	8.844e+05	9.298e+05	9.068e+05	8.843e+05
20	2.075e+06	1.976e+06	1.881e+06	2.078e+06	1.980e+06	1.886e+06
30	2.640e+06	2.456e+06	2.284e+06	2.657e+06	2.474e+06	2.304e+06
40	2.699e+06	2.427e+06	2.206e+06	2.709e+06	2.468e+06	2.248e+06
50	2.380e+06	2.115e+06	1.880e+06	2.448e+06	2.185e+06	1.949e+06
60	1.960e+06	1.703e+06	1.479e+06	2.062e+06	1.806e+06	1.582e+06
70	1.528e+06	1.299e+06	1.103e+06	1.699e+06	1.439e+06	1.242e+06
80	1.145e+06	9.512e+05	7.896e+05	1.329e+06	1.134e+06	9.709e+05
90	8.321e+05	6.758ee+05	5.485e+05	1.063e+06	9.057e+05	7.767e+05
100	5.902e+05	4.687e+05	3.719e+05	8.746e+05	7.510e+05	6.522e+05

Table 6: Numerical simulation of **A**

Time (months)	**CPC**			**Caputo**		
	$\varsigma = 0.95$	$\varsigma = 0.90$	$\varsigma = 0.85$	$\varsigma = 0.95$	$\varsigma = 0.90$	$\varsigma = 0.85$
0	5000	5000	5000	5000	5000	5000
10	1.775e+05	1.684e+05	1.596e+05	1.988e+05	1.903e+05	1.822e+05
20	5.327e+05	4.850e+05	4.414e+05	5.672e+05	5.202e+05	4.770e+05
30	7.499e+05	6.629e+05	5.862e+05	7.935e+05	7.071e+05	6.310e+05
40	8.051e+05	6.968e+05	6.038e+05	8.557e+05	7.479e+05	6.553e+05
50	7.703e+05	6.562e+05	5.599e+05	8.271e+05	7.133e+05	6.174e+05
60	6.942e+05	5.830e+05	4.904e+05	7.571e+05	6.460e+05	5.536e+05
70	6.006e+05	4.967e+05	4.114e+05	6.696e+05	5.659e+05	4.806e+05
80	5.019e+05	4.081e+05	3.322e+05	5.776e+05	4.839e+05	4.079e+05
90	4.064e+05	3.244e+05	2.591e+05	4.894e+05	4.073e+05	3.418e+05
100	3.199e+05	2.503e+05	1.959e+05	4.108e+05	3.410e+05	2.863e+05

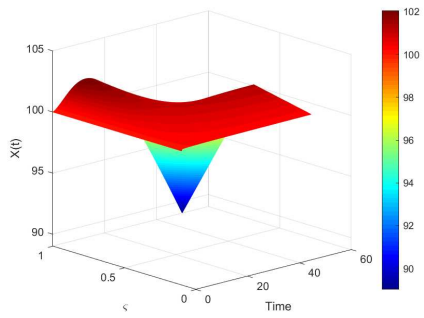

(a) 3D surface plot of **X**

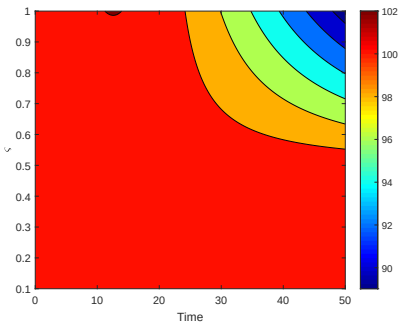

(b) Contour plot of **X**

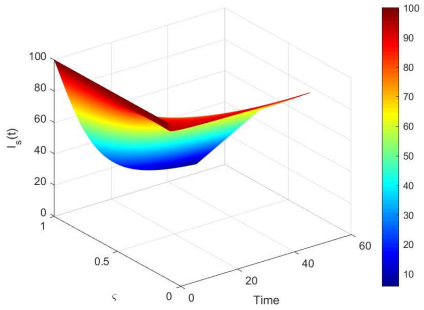

(c) 3D surface plot of $\mathbf{I_s}$

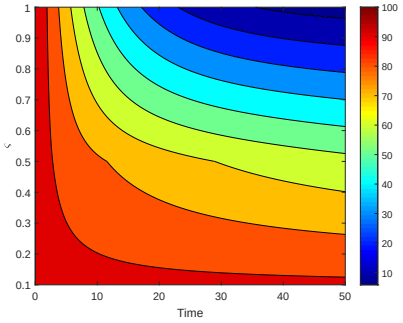

(d) Contour plot of $\mathbf{I_s}$

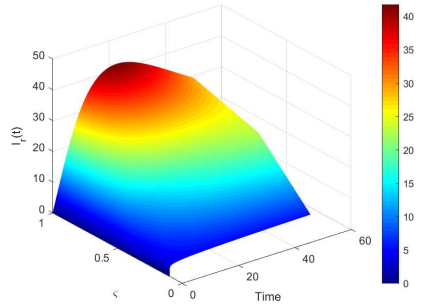

(e) 3D surface plot of $\mathbf{I_r}$

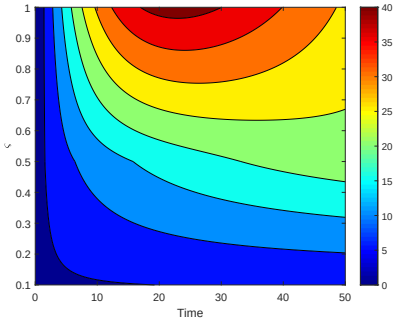

(f) Contour plot of $\mathbf{I_r}$

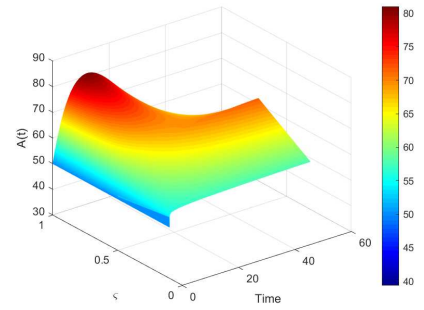

(g) 3D surface plot of **A**

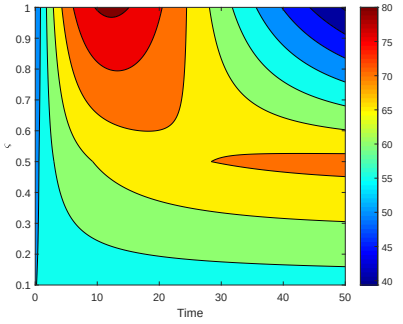

(h) Contour plot of **A**

Figure 6: 3D surface plots and contour plots at different fractional order values within feasible domain

8. Conclusion

Using a nonlinear model, this study investigates the dynamics of bacterial infections resistant to antibiotics in four groups. By offering a fractional order model that incorporates early diagnosis and prevention strategies, the study demonstrates how robust immune systems can halt the onset of disease without the need for medicine, thereby promoting disease-free environments. Solutions exhibited qualities like optimism, individuality, and existence. Both the local and global stability of the model's endemic and asymptomatic disease-free effects are examined, as well as the infection threshold of the model. LADM is a powerful analytical method for dealing with fractional order systems, providing a strong computational mechanism for understanding physical problems. Hybrid fractional operators are particularly effective in mathematical modeling of antibiotic-resistant bacterial infections, offering better capture of phenomena than the integer-order model due to its greater memory. Fractional models offer a wide range of solutions, enabling better fit between conceptual and actual data. The CPC fractional operator simulates bacterial infections, offering a realistic method for reducing antibiotic-resistant infections. Future research should focus on this technique, as it yields superior results for different fractional derivative values. As fractional values decrease, solutions become more precise and reliable, increasing the effectiveness of this method in preventing certain illnesses. The study has shortcomings, including its dependence on literature-based parameter values, lack of data fitting, and minimal generalizability. To improve future research, it is suggested to employ real-world datasets and add data-fitting techniques to increase the accuracy and broader application of the study's outcomes. Our model has limitations including a high computing cost, difficulties comprehending fractional orders, and the possibility of oversimplifying real-world complexity. However, its future potential to incorporate memory effects and non-local dynamics may improve forecast accuracy and nuanced control strategy design for bacterial infections and zoonotic diseases, resulting in a better knowledge of bacterial growth and dissemination in complicated ecosystems. Future studies should consider thorough modeling and investigate the best controls for the proposed model under the Caputo operator. By altering fractional parameters, interpretations for infection duration can be improved.

References

[1] David M Shlaes, Dale N Gerding, Joseph F John Jr, William A Craig, Donald L Bornstein, Robert A Duncan, Mark R Eckman, William E Farrer, William H Greene, Victor Lorian, et al. Society for healthcare epidemiology of america and infectious diseases society of america joint committee on the prevention of antimicrobial resistance guidelines for the prevention of antimicrobial resistance in hospitals. *Infection Control & Hospital Epidemiology*, 18(4):275–291, 1997.

[2] Marianne Frieri, Krishan Kumar, and Anthony Boutin. Antibiotic resistance. *Journal of Infection and Public Health*, 10(4):369–378, 2017.

[3] Elizabeth M Darby, Eleftheria Trampari, Pauline Siasat, Maria Solsona Gaya, Ilyas Alav, Mark A Webber, and Jessica MA Blair. Molecular mechanisms of antibiotic resistance revisited. *Nature Reviews Microbiology*, 21(5):280–295, 2023.

[4] David Chinemerem Nwobodo, Malachy Chigozie Ugwu, Clement Oliseloke Anie, Mush-

tak TS Al-Ouqaili, Joseph Chinedu Ikem, Uchenna Victor Chigozie, and Morteza Saki. Antibiotic resistance: The challenges and some emerging strategies for tackling a global menace. *Journal of Clinical Laboratory Analysis*, 36(9):e24655, 2022.

[5] Mathieu F Chellat, Luka Raguž, and Rainer Riedl. Targeting antibiotic resistance. *Angewandte Chemie International Edition*, 55(23):6600–6626, 2016.

[6] Renata Urban-Chmiel, Agnieszka Marek, Dagmara Stepień-Pyśniak, Kinga Wieczorek, Marta Dec, Anna Nowaczek, and Jacek Osek. Antibiotic resistance in bacteria: A review. *Antibiotics*, 11(8):1079, 2022.

[7] Rehab Noori Shalan, R Shireen, and Alaa Hussien Lafta. Discrete sis model with immigrants and treatment. *Journal of Interdisciplinary Mathematics*, 24(5):1201–1206, 2021.

[8] Zahraa Aamer, Shireen Jawad, Belal Batiha, Ali Hasan Ali, Firas Ghanim, and Alina Alb Lupaş. Evaluation of the dynamics of psychological panic factor, glucose risk and estrogen effects on breast cancer model. *Computation*, 12(8), 2024.

[9] Eman Hakeem, Shireen Jawad, Ali Hasan Ali, Mohamed Kallel, and Husam A Neamah. How mathematical models might predict desertification from global warming and dust pollutants. *MethodsX*, 14:103259, 2025.

[10] Nouf Alghamdi, Mal Horsburgh, and Bakhtier Vasiev. A combined experimental and mathematical study of the evolution of microbial community composed of interacting staphylococcus strains. *arXiv preprint arXiv:2402.04939*, 2024.

[11] John Fors, Natasha Strydom, William S Fox, Ron J Keizer, and Radojka M Savic. Mathematical model and tool to explore shorter multi-drug therapy options for active pulmonary tuberculosis. *PLoS Computational Biology*, 16(8):e1008107, 2020.

[12] Éva Kocsmár, György Miklós Buzás, Ildikó Szirtes, Ildikó Kocsmár, Zsófia Kramer, Attila Szijártó, Petra Fadgyas-Freyler, Kató Szénás, Massimo Rugge, Matteo Fassan, et al. Primary and secondary clarithromycin resistance in helicobacter pylori and mathematical modeling of the role of macrolides. *Nature Communications*, 12(1):2255, 2021.

[13] Joshua Kiddy K Asamoah, Farai Nyabadza, Zhen Jin, Ebenezer Bonyah, Muhammad Altaf Khan, Michael Y Li, and Tasawar Hayat. Backward bifurcation and sensitivity analysis for bacterial meningitis transmission dynamics with a nonlinear recovery rate. *Chaos, Solitons & Fractals*, 140:110237, 2020.

[14] Muhammad Farman, Rabia Sarwar, and Ali Akgül. Modeling and analysis of sustainable approach for dynamics of infections in plant virus with fractal fractional operator. *Chaos, Solitons & Fractals*, 170:113373, 2023.

[15] T J Irving, K B Blyuss, C Colijn, and C L Trotter. Modelling meningococcal meningitis in the african meningitis belt. *Epidemiology & Infection*, 140(5):897–905, 2012.

[16] Changjin Xu and Muhammad Farman. Dynamical transmission and mathematical analysis of ebola virus using a constant proportional operator with a power law kernel. *Fractal and Fractional*, 7(10):706, 2023.

[17] Ying Wang and Jiqiang Jiang. Existence and nonexistence of positive solutions for the fractional coupled system involving generalized p-laplacian. *Advances in Difference Equations*, 2017(1):337, 2017.

[18] Huiqin Zhang, Yanping Chen, Jianwei Zhou, and Yang Wang. Finite element scheme with h2n2 interpolation for multi-term time-fractional mixed sub-diffusion and diffusion-wave

equation. *Advances in Applied Mathematics and Mechanics*, 16(5):1197–1222, 2024.

[19] Bahatdin Daşbaşı. The fractional-order mathematical modeling of bacterial resistance against multiple antibiotics in case of local bacterial infection. *Sakarya University Journal of Science*, 21(3):442–453, 2017.

[20] Muhammad Farman, Ali Hasan, Muhammad Sultan, Aqeel Ahmad, Ali Akgül, Faryal Chaudhry, Mohammed Zakarya, Wedad Albalawi, and Wajaree Weera. Yellow virus epidemiological analysis in red chili plants using mittag-leffler kernel. *Alexandria Engineering Journal*, 66:811–825, 2023.

[21] Bahatdin Daşbaşı. Fractional order bacterial infection model with effects of anti-virulence drug and antibiotic. *Chaos, Solitons & Fractals*, 170:113331, 2023.

[22] Muhammad Farman, Ali Akgül, Harish Garg, Dumitru Baleanu, Evren Hincal, and Sundas Shahzeen. Mathematical analysis and dynamical transmission of monkeypox virus model with fractional operator. *Expert Systems*, 42(1):e13475, 2025.

[23] Muhammad Farman, Kottakkaran Sooppy Nisar, Aamir Shehzad, Dumitru Baleanu, Ayesha Amjad, and Faisal Sultan. Computational analysis and chaos control of the fractional order syphilis disease model through modeling. *Ain Shams Engineering Journal*, 15(6):102743, 2024.

[24] Muhammad Farman, Nezihal Gokbulut, Ulas Hurdoganoglu, Evren Hincal, and Kaya Suer. Fractional order model of mrsa bacterial infection with real data fitting: Computational analysis and modeling. *Computers in Biology and Medicine*, 173:108367, 2024.

[25] Ana PS Koltun, José Trobia, Antonio M Batista, Ervin K Lenzi, Moises S Santos, Fernando S Borges, Kelly C Iarosz, Iberê L Caldas, and Enrique C Gabrick. Fractional tumour-immune model with drug resistance. *Brazilian Journal of Physics*, 54(2):41, 2024.

[26] Nahaa E. Alsubaie, Fathelrhman EL Guma, Kaouther Boulehmi, Naseam Al-kuleab, and Mohamed A. Abdoon. Improving influenza epidemiological models under caputo fractional-order calculus. *Symmetry*, 16(7):929, 2024.

[27] Sana Abdulkream Alharbi, Mohamed A. Abdoon, Rania Saadeh, Reima Daher Alsemiry, Reem Allogmany, Mohammed Berir, and Fathelrhman EL Guma. Modeling and analysis of visceral leishmaniasis dynamics using fractional-order operators: A comparative study. *Mathematical Methods in the Applied Sciences*, 47(12):9918–9937, 2024.

[28] Sana Abdulkream Alharbi, Mohamed A Abdoon, Abdoelnaser M Degoot, Reima Daher Alsemiry, Reem Allogmany, Fathelrhman EL Guma, and Mohammed Berir. Mathematical modeling of influenza dynamics: A novel approach with sveihr and fractional calculus. *International Journal of Biomathematics*, page 2450147, 2025.

[29] Dumitru Baleanu, Arran Fernandez, and Ali Akgül. On a fractional operator combining proportional and classical differintegrals. *Mathematics*, 8(3):360, 2020.

[30] Ali Akgül. Some fractional derivatives with different kernels. *International Journal of Applied and Computational Mathematics*, 8(4):183, 2022.

[31] Muhammad Farman, Cicik Alfiniyah, and Aamir Shehzad. Modelling and analysis tuberculosis (tb) model with hybrid fractional operator. *Alexandria Engineering Journal*, 72:463–478, 2023.

[32] Parvaiz Ahmad Naik, Anum Zehra, Muhammad Farman, Aamir Shehzad, Sundas Shahzeen, and Zhengxin Huang. Forecasting and dynamical modeling of reversible enzymatic reactions

with a hybrid proportional fractional derivative. *Frontiers in Physics*, 11:1307307, 2024.

[33] Kottakkaran Sooppy Nisar, Muhammad Farman, Evren Hincal, and Aamir Shehzad. Modelling and analysis of bad impact of smoking in society with constant proportional-caputo fabrizio operator. *Chaos, Solitons & Fractals*, 172:113549, 2023.

[34] Changjin Xu and Muhammad Farman. Dynamical transmission and mathematical analysis of ebola virus using a constant proportional operator with a power law kernel. *Fractal and Fractional*, 7(10):706, 2023.

[35] Changpin Li, Deliang Qian, and YangQuan Chen. On riemann-liouville and caputo derivatives. *Discrete Dynamics in Nature and Society*, 2011(1):562494, 2011.

[36] Josiah Mushanyu. Mathematical modelling of community acquired antibiotic resistant infections. *Informatics in Medicine Unlocked*, 45:101452, 2024.